PAPER

Analysis and Minimization of Roundoff Noise for Generalized Direct-Form II Realization of 2-D Separable-Denominator Filters

Takao HINAMOTO[†a)], ***Fellow***, **Akimitsu DOI**[††b)], ***Member***, ***and*** **Wu-Sheng LU**[†††c)], ***Nonmember***

SUMMARY Based on the concept of polynomial operators, this paper explores generalized direct-form II structure and its state-space realization for two-dimensional separable-denominator digital filters of order (m, n) where a structure with $3(m+n)+mn+1$ fixed parameters plus $m+n$ free parameters is introduced and analyzed. An l_2-scaling method utilizing different coupling coefficients at different branch nodes to avoid overflow is presented. Expressions of evaluating the roundoff noise for the filter structure as well as its state-space realization are derived and investigated. The availability of the $m+n$ free parameters is shown to be beneficial as the roundoff noise measures can be minimized with respect to these free parameters by means of an exhaustive search over a set with finite number of candidate elements. The important role these parameters can play in the endeavors of roundoff noise reduction is demonstrated by numerical experiments.

key words: *generalized direct-form II, polynomial operator, realization, roundoff noise, 2-D separable-denominator digital filter*

1. Introduction

Two-dimensional (2-D) separable-denominator digital filters are recognized as a very popular class of multidimensional signal processors because it meets the need for simple and stable system structure with desirable symmetric properties for economical implementation [1]–[8]. On the other hand, delta-operator-based design and implementation for digital signal processing and control systems have been extensively studied [9]–[18], demonstrating excellent finite-word-length (FWL) performance under fast sampling. In particular, a new structure based on the concept of polynomial operators has been explored for digital filter implementation [14]. This new structure can be viewed as a generalization of the shift operator z-based direct-form II transposed structure. Other issue important for implementing IIR digital filters with fixed-point arithmetic is the reduction of roundoff noise. Studies on this topic include the synthesis of 2-D state-space filter structures with minimum roundoff noise in [19], [20] and the minimization of roundoff noise using delta-operator realization [21] or applying jointly optimal high-order error feedback and realization [22], [23]. Note that quantizations were carried out *after* multiplications in [19], [20], whereas in [22], [23] they were performed *before* multiplications.

In this paper, motivated by [13], [14] and based on the concept of polynomial operators, two sets of operators are introduced and it is shown that 2-D separable-denominator digital filters can be expressed by a generalized SIMO direct-form II and a generalized MISO transposed direct-form II in cascade. This filter structure is then realized by Roesser's local state-space model with very sparse parameters, and l_2-scaling is performed by using different coupling coefficients at different branch nodes to avoid overflow. Expressions of evaluating the roundoff noise for generalized direct-form II structure and its state-space realization are derived and investigated. It is clarified that in a generalized direct-form II structure and its state-space realization the roundoff noise measures are explicit functions of $m+n$ free parameters. As a result of this parameterization, performance of the digital filter involved may be improved or optimized by tuning these parameters to reduce or minimize a chosen measure. In effect, in the scenario where the free parameters are subject to FWL format for actual implementation, it is shown that each roundoff noise measure can be minimized with respect to the free parameters subject to l_2-scaling constraints by an exhaustive search of a set with finite number of candidate elements. A numerical example is presented to demonstrate the important role these parameters can play in the endeavors of roundoff noise reduction as well as the validity and effectiveness of the proposed techniques. The present paper can be viewed as a unified version of our work in [24], [25].

2. Realization of 2-D Digital Filters

2.1 Structural Transformation

Consider a 2-D stable separable-denominator digital filter of order (m, n) described by

$$H(z_1, z_2) = \frac{\displaystyle\sum_{k=0}^{m}\sum_{l=0}^{n} c_{kl} z_1^{m-k} z_2^{n-l}}{\left(z_1^m + \displaystyle\sum_{k=1}^{m} a_k z_1^{m-k}\right)\left(z_2^n + \displaystyle\sum_{l=1}^{n} b_l z_2^{n-l}\right)} \tag{1}$$

where the denominator and numerator are assumed coprime. Let $\boldsymbol{P}_1$ and $\boldsymbol{P}_2$ be $(m+1)\times(m+1)$ and $(n+1)\times(n+1)$ nonsingular matrices, respectively, defined by

Manuscript received November 4, 2019.
Manuscript revised February 27, 2020.

[†]The author is with Hiroshima University, Higashihiroshima-shi, 739-8527 Japan.
[††]The author is with Faculty of Applied Information Science, Hiroshima Institute of Technology, Hiroshima-shi, 731-5193 Japan.
[†††]The author is with the Department of Electrical and Computer Engineering, University of Victoria, Victoria, B.C., V8W 3P6, Canada.
a) E-mail: hinamoto@ieee.org
b) E-mail: doi@cc.it-hiroshima.ac.jp
c) E-mail: wslu@ece.uvic.ca

DOI: 10.1587/transfun.2019EAP1152

$$\begin{bmatrix} q_0^h(z_1) \\ q_1^h(z_1) \\ \vdots \\ q_m^h(z_1) \end{bmatrix} = \boldsymbol{P}_1 \begin{bmatrix} z_1^m \\ \vdots \\ z_1 \\ 1 \end{bmatrix}, \quad \begin{bmatrix} q_0^v(z_2) \\ q_1^v(z_2) \\ \vdots \\ q_n^v(z_2) \end{bmatrix} = \boldsymbol{P}_2 \begin{bmatrix} z_2^n \\ \vdots \\ z_2 \\ 1 \end{bmatrix} \tag{2}$$

where quantities $q_k^h(z_1)$ for $k = 0, 1, \cdots, m$ and $q_l^v(z_2)$ for $l = 0, 1, \cdots, n$ are defined as horizontal and vertical polynomial operators, respectively.

Next, we define scalars $\{\alpha_k | \, k = 1, 2, \cdots, m\}$, $\{\beta_l | \, l = 1, 2, \cdots, n\}$ and $\{r_{kl} | \, k = 0, 1, \cdots, m; \; l = 0, 1, \cdots, n\}$ so that

$$\begin{aligned} &\kappa_1 \begin{bmatrix} 1 & \alpha_1 & \alpha_2 & \cdots & \alpha_m \end{bmatrix} \boldsymbol{P}_1 = \begin{bmatrix} 1 & a_1 & a_2 & \cdots & a_m \end{bmatrix} \\ &\kappa_2 \begin{bmatrix} 1 & \beta_1 & \beta_2 & \cdots & \beta_n \end{bmatrix} \boldsymbol{P}_2 = \begin{bmatrix} 1 & b_1 & b_2 & \cdots & b_n \end{bmatrix} \\ &\kappa_1 \kappa_2 \boldsymbol{P}_1^T \begin{bmatrix} r_{00} & \cdots & r_{0n} \\ \vdots & \ddots & \vdots \\ r_{m0} & \cdots & r_{mn} \end{bmatrix} \boldsymbol{P}_2 = \begin{bmatrix} c_{00} & \cdots & c_{0n} \\ \vdots & \ddots & \vdots \\ c_{m0} & \cdots & c_{mn} \end{bmatrix} \end{aligned} \tag{3}$$

where κ_1 and κ_2 are scaling factors to be specified shortly. From (1)–(3), it can readily be verified that the transfer function in (1) can be expressed as

$$H(z_1, z_2) = \frac{\displaystyle\sum_{k=0}^{m} \sum_{l=0}^{n} r_{kl} q_k^h(z_1) q_l^v(z_2)}{\Big(q_0^h(z_1) + \displaystyle\sum_{k=1}^{m} \alpha_k q_k^h(z_1)\Big)\Big(q_0^v(z_2) + \displaystyle\sum_{l=1}^{n} \beta_l q_l^v(z_2)\Big)} \tag{4}$$

where κ_1 and κ_2 are determined by requiring the coefficient of $q_0^h(z_1)$ and that of $q_0^v(z_2)$ to be unity, respectively.

Equation (4) shows that the filter can be parameterized by scalars $\{\alpha_k | \, k = 1, 2, \cdots, m\}$, $\{\beta_l | \, l = 1, 2, \cdots, n\}$ and $\{r_{kl} | \, k = 0, 1, \cdots, m; \; l = 0, 1, \cdots, n\}$ provided that the horizontal and vertical polynomial operators: $\{q_k^h(z_1) | \, k = 0, 1, \cdots, m\}$ and $\{q_l^v(z_2) | \, l = 0, 1, \cdots, n\}$ are specified with the particular application.

We now consider two sets of polynomial operators which, as we shall see shortly, lead to a useful structure for filter implementation. To this end we define

$$\begin{aligned} \rho_k^h(z_1) &= \frac{z_1 - \overline{\gamma}_k}{\overline{\Delta}_k} \quad \text{for} \quad k = 1, 2, \cdots, m \\ \rho_l^v(z_2) &= \frac{z_2 - \hat{\gamma}_l}{\hat{\Delta}_l} \quad \text{for} \quad l = 1, 2, \cdots, n \end{aligned} \tag{5}$$

where $\{\overline{\gamma}_k\}$, $\{\hat{\gamma}_l\}$, $\{\overline{\Delta}_k > 0\}$ and $\{\hat{\Delta}_l > 0\}$ are four sets of constants to be examined later, and let the polynomial operators be in the form

$$\begin{aligned} &q_k^h(z_1) = \rho_{k+1}^h(z_1) \rho_{k+2}^h(z_1) \cdots \rho_m^h(z_1), \quad k = 0, 1, \cdots, m-1 \\ &q_l^v(z_2) = \rho_{l+1}^v(z_2) \rho_{l+2}^v(z_2) \cdots \rho_n^v(z_2), \quad l = 0, 1, \cdots, n-1 \\ &q_m^h(z_1) = q_n^v(z_2) = 1 \end{aligned} \tag{6}$$

which are equivalent to

$$\begin{aligned} &\begin{bmatrix} q_0^h(z_1) \\ \vdots \\ q_{m-1}^h(z_1) \\ q_m^h(z_1) \end{bmatrix} = \begin{bmatrix} \rho_1^h(z_1) \rho_2^h(z_1) \cdots \rho_m^h(z_1) \\ \vdots \\ \rho_m^h(z_1) \\ 1 \end{bmatrix} = \boldsymbol{P}_1 \begin{bmatrix} z_1^m \\ \vdots \\ z_1 \\ 1 \end{bmatrix} \\ &\begin{bmatrix} q_0^v(z_2) \\ \vdots \\ q_{n-1}^v(z_2) \\ q_n^v(z_2) \end{bmatrix} = \begin{bmatrix} \rho_1^v(z_2) \rho_2^v(z_2) \cdots \rho_n^v(z_2) \\ \vdots \\ \rho_n^v(z_2) \\ 1 \end{bmatrix} = \boldsymbol{P}_2 \begin{bmatrix} z_2^n \\ \vdots \\ z_2 \\ 1 \end{bmatrix} \end{aligned} \tag{7}$$

As an example, we consider the case where $(m, n) = (3, 3)$. Then we have

$$\begin{aligned} \boldsymbol{P}_1 &= \frac{1}{\overline{\Delta}_1 \overline{\Delta}_2 \overline{\Delta}_3} \\ &\cdot \begin{bmatrix} 1 & -(\overline{\gamma}_1 + \overline{\gamma}_2 + \overline{\gamma}_3) & \overline{\gamma}_1 \overline{\gamma}_2 + \overline{\gamma}_2 \overline{\gamma}_3 + \overline{\gamma}_3 \overline{\gamma}_1 & -\overline{\gamma}_1 \overline{\gamma}_2 \overline{\gamma}_3 \\ 0 & \overline{\Delta}_1 & -(\overline{\gamma}_2 + \overline{\gamma}_3) \overline{\Delta}_1 & \overline{\gamma}_2 \overline{\gamma}_3 \overline{\Delta}_1 \\ 0 & 0 & \overline{\Delta}_1 \overline{\Delta}_2 & -\overline{\gamma}_3 \overline{\Delta}_1 \overline{\Delta}_2 \\ 0 & 0 & 0 & \overline{\Delta}_1 \overline{\Delta}_2 \overline{\Delta}_3 \end{bmatrix} \\ \boldsymbol{P}_2 &= \frac{1}{\hat{\Delta}_1 \hat{\Delta}_2 \hat{\Delta}_3} \\ &\cdot \begin{bmatrix} 1 & -(\hat{\gamma}_1 + \hat{\gamma}_2 + \hat{\gamma}_3) & \hat{\gamma}_1 \hat{\gamma}_2 + \hat{\gamma}_2 \hat{\gamma}_3 + \hat{\gamma}_3 \hat{\gamma}_1 & -\hat{\gamma}_1 \hat{\gamma}_2 \hat{\gamma}_3 \\ 0 & \hat{\Delta}_1 & -(\hat{\gamma}_2 + \hat{\gamma}_3) \hat{\Delta}_1 & \hat{\gamma}_2 \hat{\gamma}_3 \hat{\Delta}_1 \\ 0 & 0 & \hat{\Delta}_1 \hat{\Delta}_2 & -\hat{\gamma}_3 \hat{\Delta}_1 \hat{\Delta}_2 \\ 0 & 0 & 0 & \hat{\Delta}_1 \hat{\Delta}_2 \hat{\Delta}_3 \end{bmatrix} \end{aligned} \tag{8}$$

Hence, by using (5), we can specify the corresponding transformation matrices $\boldsymbol{P}_1$, $\boldsymbol{P}_2$ and scalars $\kappa_1 = \overline{\Delta}_1 \overline{\Delta}_2 \cdots \overline{\Delta}_m$, $\kappa_2 = \hat{\Delta}_1 \hat{\Delta}_2 \cdots \hat{\Delta}_n$. From (6), it follows that for $k, l \geq 1$,

$$\begin{aligned} \frac{q_k^h(z_1)}{q_0^h(z_1)} &= \frac{\rho_{k+1}^h(z_1) \rho_{k+2}^h(z_1) \cdots \rho_m^h(z_1)}{\rho_1^h(z_1) \rho_2^h(z_1) \cdots \rho_m^h(z_1)} \\ &= \rho_1^h(z_1)^{-1} \rho_2^h(z_1)^{-1} \cdots \rho_k^h(z_1)^{-1} \\ \frac{q_l^v(z_2)}{q_0^v(z_2)} &= \frac{\rho_{l+1}^v(z_2) \rho_{l+2}^v(z_2) \cdots \rho_n^v(z_2)}{\rho_1^v(z_2) \rho_2^v(z_2) \cdots \rho_n^v(z_2)} \\ &= \rho_1^v(z_2)^{-1} \rho_2^v(z_2)^{-1} \cdots \rho_l^v(z_2)^{-1} \end{aligned} \tag{9}$$

This leads to a useful expression of the transfer function in (4) as

$$H(z_1, z_2) = \frac{\displaystyle\sum_{k=0}^{m} \sum_{l=0}^{n} r_{kl} \prod_{p=0}^{k} \rho_p^h(z_1)^{-1} \prod_{q=0}^{l} \rho_q^v(z_2)^{-1}}{\Big(\displaystyle\sum_{k=0}^{m} \alpha_k \prod_{p=0}^{k} \rho_p^h(z_1)^{-1}\Big)\Big(\displaystyle\sum_{l=0}^{n} \beta_l \prod_{q=0}^{l} \rho_q^v(z_2)^{-1}\Big)} \tag{10}$$

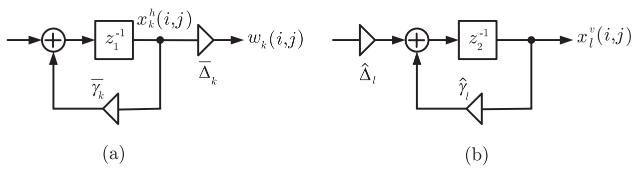

Fig. 1 (a) Implementation of $\rho_k^h(z_1)^{-1}$ and (b) that of $\rho_l^v(z_2)^{-1}$.

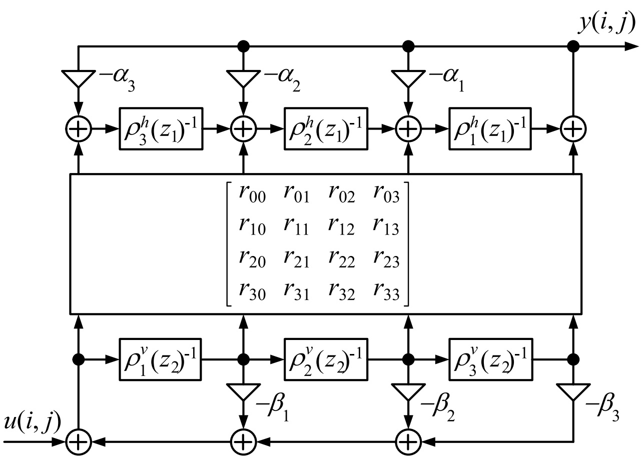

Fig. 2 The 2-D filter structure of (2) with $(m, n) = (3, 3)$.

where $\alpha_0 = \beta_0 = 1$ and $\rho_0^h(z_1)^{-1} = \rho_0^v(z_2)^{-1} = 1$.

Implementations of $\rho_k^h(z_1)^{-1}$ and $\rho_l^v(z_2)^{-1}$ are depicted in Fig. 1. As an illustrative example, the structure of (10) for a 2-D filter with $(m, n) = (3, 3)$ is depicted in Fig. 2 where $u(i, j)$ is a scalar input and $y(i, j)$ is a scalar output.

From Figs. 1 and 2, we deduce

$$
\begin{aligned}
y(i,j) &= w_1(i,j) + \sum_{l=1}^{n} r_{0l} x_l^v(i,j) \\
&\quad + r_{00}\Big[u(i,j) - \sum_{l=1}^{n} \beta_l x_l^v(i,j)\Big] \\
w_k(i,j) &= \rho_k^h(z_1)^{-1}\Big\{w_{k+1}(i,j) + \sum_{l=1}^{n} r_{kl} x_l^v(i,j) \\
&\quad + r_{k0}\Big[u(i,j) - \sum_{l=1}^{n} \beta_l x_l^v(i,j)\Big] - \alpha_k y(i,j)\Big\}
\end{aligned}
\tag{11}
$$

where $k = 1, 2, \cdots, m$ and $w_{m+1}(i, j) = 0$. In addition,

$$
\begin{aligned}
x_1^v(i,j+1) &= \hat{\gamma}_1 x_1^v(i,j) + \hat{\Delta}_1\Big[u(i,j) - \sum_{l=1}^{n} \beta_l x_l^v(i,j)\Big] \\
x_l^v(i,j+1) &= \hat{\Delta}_l x_{l-1}^v(i,j) + \hat{\gamma}_l x_l^v(i,j) \ \text{for } l = 2, 3, \cdots, n
\end{aligned}
\tag{12}
$$

The availability of these additional free parameters makes it possible to further reduce the FWL effects and, as will be demonstrated in the simulations of Sect. 4, the extra reduction can be quite significant.

In what follows, the minimization of roundoff noise measure is carried out in a local state-space setting, and we start by deriving Roesser's state-space model for the 2-D filter in (10).

2.2 Local State-Space Realization

From (5), the second equation in (11) can be written as

$$
\begin{aligned}
w_k(i,j) = \frac{\overline{\Delta}_k}{z_1 - \overline{\gamma}_k}\Big\{ & w_{k+1}(i,j) + \sum_{l=1}^{n} r_{kl} x_l^v(i,j) \\
& + r_{k0}\Big[u(i,j) - \sum_{l=1}^{n} \beta_l x_l^v(i,j)\Big] - \alpha_k y(i,j)\Big\}
\end{aligned}
\tag{13a}
$$

which leads to

$$
\begin{aligned}
(z_1 - \overline{\gamma}_k) x_k^h(i,j) &= \overline{\Delta}_{k+1} x_{k+1}^h(i,j) + \sum_{l=1}^{n} r_{kl} x_l^v(i,j) \\
&\quad + r_{k0}\Big[u(i,j) - \sum_{l=1}^{n} \beta_l x_l^v(i,j)\Big] \\
&\quad - \alpha_k \Big\{\overline{\Delta}_1 x_1^h(i,j) + \sum_{l=1}^{n} r_{0l} x_l^v(i,j) \\
&\quad + r_{00}\Big[u(i,j) - \sum_{l=1}^{n} \beta_l x_l^v(i,j)\Big]\Big\}
\end{aligned}
\tag{13b}
$$

or, equivalently

$$
\begin{aligned}
x_k^h(i+1,j) &= -\alpha_k \overline{\Delta}_1 x_1^h(i,j) + \overline{\Delta}_{k+1} x_{k+1}^h(i,j) + \overline{\gamma}_k x_k^h(i,j) \\
&\quad + \sum_{l=1}^{n} (r_{kl} - \alpha_k r_{0l} - r_{k0}\beta_l + r_{00}\alpha_k \beta_l) x_l^v(i,j) \\
&\quad + (r_{k0} - r_{00}\alpha_k) u(i,j)
\end{aligned}
\tag{13c}
$$

where $k = 1, 2, \cdots, m$ and $x_{m+1}^h(i, j) = 0$.

From the first equation in (11), (12) and (13c), the transfer function $H(z_1, z_2)$ in (10) can be realized by the Roesser local state-space model [26], [27] as

$$
\begin{aligned}
\begin{bmatrix} \boldsymbol{x}^h(i+1,j) \\ \boldsymbol{x}^v(i,j+1) \end{bmatrix} &= \begin{bmatrix} \boldsymbol{A}_1 & \boldsymbol{A}_2 \\ \boldsymbol{0} & \boldsymbol{A}_4 \end{bmatrix} \begin{bmatrix} \boldsymbol{x}^h(i,j) \\ \boldsymbol{x}^v(i,j) \end{bmatrix} + \begin{bmatrix} \boldsymbol{b}_1 \\ \boldsymbol{b}_2 \end{bmatrix} u(i,j) \\
y(i,j) &= \begin{bmatrix} \boldsymbol{c}_1 & \boldsymbol{c}_2 \end{bmatrix} \begin{bmatrix} \boldsymbol{x}^h(i,j) \\ \boldsymbol{x}^v(i,j) \end{bmatrix} + d\, u(i,j)
\end{aligned}
\tag{14}
$$

where $\boldsymbol{x}^h(i, j)$ is an $m \times 1$ horizontal state vector and $\boldsymbol{x}^v(i, j)$ is an $n \times 1$ vertical state vector, defined by

$$
\boldsymbol{x}^h(i,j) = \begin{bmatrix} x_1^h(i,j) \\ x_2^h(i,j) \\ \vdots \\ x_m^h(i,j) \end{bmatrix}, \qquad \boldsymbol{x}^v(i,j) = \begin{bmatrix} x_1^v(i,j) \\ x_2^v(i,j) \\ \vdots \\ x_n^v(i,j) \end{bmatrix}
$$

and the coefficient matrices are given by

$$\boldsymbol{A}_1 = \begin{bmatrix} -\alpha_1\overline{\Delta}_1 & \overline{\Delta}_2 & \cdots & 0 \\ -\alpha_2\overline{\Delta}_1 & 0 & \ddots & \vdots \\ \vdots & \vdots & \ddots & \overline{\Delta}_m \\ -\alpha_m\overline{\Delta}_1 & 0 & \cdots & 0 \end{bmatrix} + \begin{bmatrix} \overline{\gamma}_1 & 0 & \cdots & 0 \\ 0 & \overline{\gamma}_2 & \ddots & \vdots \\ \vdots & \ddots & \ddots & 0 \\ 0 & \cdots & 0 & \overline{\gamma}_m \end{bmatrix}$$

$$\boldsymbol{A}_2 = \begin{bmatrix} r_{11} & r_{12} & \cdots & r_{1n} \\ r_{21} & r_{22} & \cdots & r_{2n} \\ \vdots & \vdots & \ddots & \vdots \\ r_{m1} & r_{m2} & \cdots & r_{mn} \end{bmatrix} - \begin{bmatrix} \alpha_1 \\ \alpha_2 \\ \vdots \\ \alpha_m \end{bmatrix} \begin{bmatrix} r_{01} & r_{02} & \cdots & r_{0n} \end{bmatrix}$$
$$- \begin{bmatrix} r_{10} \\ r_{20} \\ \vdots \\ r_{m0} \end{bmatrix} \begin{bmatrix} \beta_1 & \beta_2 & \cdots & \beta_n \end{bmatrix} + r_{00} \begin{bmatrix} \alpha_1 \\ \alpha_2 \\ \vdots \\ \alpha_m \end{bmatrix} \begin{bmatrix} \beta_1 & \beta_2 & \cdots & \beta_n \end{bmatrix}$$

$$\boldsymbol{A}_4 = \begin{bmatrix} -\beta_1\hat{\Delta}_1 & -\beta_2\hat{\Delta}_1 & \cdots & -\beta_n\hat{\Delta}_1 \\ \hat{\Delta}_2 & 0 & \cdots & 0 \\ \vdots & \ddots & \ddots & \vdots \\ 0 & \cdots & \hat{\Delta}_n & 0 \end{bmatrix} + \begin{bmatrix} \hat{\gamma}_1 & 0 & \cdots & 0 \\ 0 & \hat{\gamma}_2 & \ddots & \vdots \\ \vdots & \ddots & \ddots & 0 \\ 0 & \cdots & 0 & \hat{\gamma}_n \end{bmatrix}$$

$$\boldsymbol{b}_1 = \begin{bmatrix} r_{10} \\ r_{20} \\ \vdots \\ r_{m0} \end{bmatrix} - r_{00} \begin{bmatrix} \alpha_1 \\ \alpha_2 \\ \vdots \\ \alpha_m \end{bmatrix}, \qquad \boldsymbol{b}_2 = \begin{bmatrix} \hat{\Delta}_1 \\ 0 \\ \vdots \\ 0 \end{bmatrix}$$
$$\boldsymbol{c}_1 = \begin{bmatrix} \overline{\Delta}_1 & 0 & \cdots & 0 \end{bmatrix}, \qquad d = r_{00}$$
$$\boldsymbol{c}_2 = \begin{bmatrix} r_{01} & r_{02} & \cdots & r_{0n} \end{bmatrix} - r_{00} \begin{bmatrix} \beta_1 & \beta_2 & \cdots & \beta_n \end{bmatrix}$$

The transfer function of the local state-space model in (14) is then expressed in terms of state-space parameters as [27]

$$\begin{aligned} H(z_1, z_2) &= \begin{bmatrix} \boldsymbol{c}_1 & \boldsymbol{c}_2 \end{bmatrix} \begin{bmatrix} z_1\boldsymbol{I}_m - \boldsymbol{A}_1 & -\boldsymbol{A}_2 \\ \boldsymbol{0} & z_2\boldsymbol{I}_n - \boldsymbol{A}_4 \end{bmatrix}^{-1} \begin{bmatrix} \boldsymbol{b}_1 \\ \boldsymbol{b}_2 \end{bmatrix} + d \\ &= \boldsymbol{c}_1(z_1\boldsymbol{I}_m - \boldsymbol{A}_1)^{-1}\boldsymbol{b}_1 + d \\ &\quad + [\boldsymbol{c}_1(z_1\boldsymbol{I}_m - \boldsymbol{A}_1)^{-1}\boldsymbol{A}_2 + \boldsymbol{c}_2](z_2\boldsymbol{I}_n - \boldsymbol{A}_4)^{-1}\boldsymbol{b}_2 \end{aligned} \tag{15}$$

2.3 Equivalent Local State-Space Realization

We now consider a realization with $\overline{\Delta}_k = 1$ for $k = 1, 2, \cdots, m$ and $\hat{\Delta}_l = 1$ for $l = 1, 2, \cdots, n$ in (5), which leads to a realization of the form

$$\begin{aligned} \begin{bmatrix} \tilde{\boldsymbol{x}}^h(i+1, j) \\ \tilde{\boldsymbol{x}}^v(i, j+1) \end{bmatrix} &= \begin{bmatrix} \tilde{\boldsymbol{A}}_1 & \tilde{\boldsymbol{A}}_2 \\ \boldsymbol{0} & \tilde{\boldsymbol{A}}_4 \end{bmatrix} \begin{bmatrix} \tilde{\boldsymbol{x}}^h(i, j) \\ \tilde{\boldsymbol{x}}^v(i, j) \end{bmatrix} + \begin{bmatrix} \tilde{\boldsymbol{b}}_1 \\ \tilde{\boldsymbol{b}}_2 \end{bmatrix} u(i, j) \\ y(i, j) &= \begin{bmatrix} \tilde{\boldsymbol{c}}_1 & \tilde{\boldsymbol{c}}_2 \end{bmatrix} \begin{bmatrix} \tilde{\boldsymbol{x}}^h(i, j) \\ \tilde{\boldsymbol{x}}^v(i, j) \end{bmatrix} + \tilde{d}u(i, j) \end{aligned} \tag{16}$$

where

$$\tilde{\boldsymbol{A}}_1 = \begin{bmatrix} -\tilde{\alpha}_1 & & & \\ -\tilde{\alpha}_2 & & \boldsymbol{I}_{m-1} & \\ \vdots & & & \\ -\tilde{\alpha}_m & 0 & \cdots & 0 \end{bmatrix} + \begin{bmatrix} \overline{\gamma}_1 & 0 & \cdots & 0 \\ 0 & \overline{\gamma}_2 & \ddots & \vdots \\ \vdots & \ddots & \ddots & \vdots \\ 0 & \cdots & 0 & \overline{\gamma}_m \end{bmatrix}$$

$$\tilde{\boldsymbol{A}}_4 = \begin{bmatrix} -\tilde{\beta}_1 & -\tilde{\beta}_2 & \cdots & -\tilde{\beta}_n \\ & & & 0 \\ & \boldsymbol{I}_{n-1} & & \vdots \\ & & & 0 \end{bmatrix} + \begin{bmatrix} \hat{\gamma}_1 & 0 & \cdots & 0 \\ 0 & \hat{\gamma}_2 & \ddots & \vdots \\ \vdots & \ddots & \ddots & \vdots \\ 0 & \cdots & 0 & \hat{\gamma}_n \end{bmatrix}$$

$$\tilde{\boldsymbol{b}}_2 = \begin{bmatrix} 1 & 0 & \cdots & 0 \end{bmatrix}^T, \qquad \tilde{\boldsymbol{c}}_1 = \begin{bmatrix} 1 & 0 & \cdots & 0 \end{bmatrix}$$

and coefficient matrices $\tilde{\boldsymbol{A}}_2$, $\tilde{\boldsymbol{b}}_1$, $\tilde{\boldsymbol{c}}_2$ and $\tilde{d}$ can be derived from $\{\tilde{r}_{kl} \,|\, k = 0, 1, \cdots, m;\ l = 0, 1, \cdots, n\}$, $\{\tilde{\alpha}_k \,|\, k = 1, 2, \cdots, m\}$ and $\{\tilde{\beta}_l \,|\, l = 1, 2, \cdots, n\}$ in the same manner as in (14).

Now if the state-space model in (14) is related to that in (16) by

$$\begin{bmatrix} \tilde{\boldsymbol{x}}^h(i, j) \\ \tilde{\boldsymbol{x}}^v(i, j) \end{bmatrix} = \begin{bmatrix} \boldsymbol{T}_1 & \boldsymbol{0} \\ \boldsymbol{0} & \boldsymbol{T}_4 \end{bmatrix}^{-1} \begin{bmatrix} \boldsymbol{x}^h(i, j) \\ \boldsymbol{x}^v(i, j) \end{bmatrix} \tag{17}$$

with

$$\boldsymbol{T}_1 = \mathrm{diag}\{\bar{t}_1\ \bar{t}_2\ \cdots\ \bar{t}_m\}, \qquad \boldsymbol{T}_4 = \mathrm{diag}\{\hat{t}_1\ \hat{t}_2\ \cdots\ \hat{t}_n\}$$

the relationship between the two models is found to be

$$\begin{aligned} &\tilde{\boldsymbol{A}}_1 = \boldsymbol{T}_1^{-1}\boldsymbol{A}_1\boldsymbol{T}_1, \quad &\tilde{\boldsymbol{b}}_1 = \boldsymbol{T}_1^{-1}\boldsymbol{b}_1, \quad &\tilde{\boldsymbol{c}}_1 = \boldsymbol{c}_1\boldsymbol{T}_1 \\ &\tilde{\boldsymbol{A}}_4 = \boldsymbol{T}_4^{-1}\boldsymbol{A}_4\boldsymbol{T}_4, \quad &\tilde{\boldsymbol{b}}_2 = \boldsymbol{T}_4^{-1}\boldsymbol{b}_2, \quad &\tilde{\boldsymbol{c}}_2 = \boldsymbol{c}_2\boldsymbol{T}_4 \\ &\tilde{\boldsymbol{A}}_2 = \boldsymbol{T}_1^{-1}\boldsymbol{A}_2\boldsymbol{T}_4, \quad &\tilde{d} = d & \end{aligned} \tag{18}$$

By virtue of $\tilde{\boldsymbol{c}}_1 = \boldsymbol{c}_1\boldsymbol{T}_1$, $\boldsymbol{T}_1\tilde{\boldsymbol{A}}_1 = \boldsymbol{A}_1\boldsymbol{T}_1$, $\tilde{\boldsymbol{b}}_2 = \boldsymbol{T}_4^{-1}\boldsymbol{b}_2$, $\tilde{\boldsymbol{A}}_4\boldsymbol{T}_4^{-1} = \boldsymbol{T}_4^{-1}\boldsymbol{A}_4$ and $\tilde{\boldsymbol{A}}_2 = \boldsymbol{T}_1^{-1}\boldsymbol{A}_2\boldsymbol{T}_4$ it follows that

$$\begin{aligned} \boldsymbol{T}_1^{-1} &= \mathrm{diag}\{\overline{\Delta}_1,\ \overline{\Delta}_1\overline{\Delta}_2,\ \cdots,\ \overline{\Delta}_1\overline{\Delta}_2\cdots\overline{\Delta}_m\} \\ \boldsymbol{T}_4 &= \mathrm{diag}\{\hat{\Delta}_1,\ \hat{\Delta}_1\hat{\Delta}_2,\ \cdots,\ \hat{\Delta}_1\hat{\Delta}_2\cdots\hat{\Delta}_n\} \end{aligned}$$
$$\begin{bmatrix} \tilde{\alpha}_1 \\ \tilde{\alpha}_2 \\ \vdots \\ \tilde{\alpha}_m \end{bmatrix} = \boldsymbol{T}_1^{-1} \begin{bmatrix} \alpha_1 \\ \alpha_2 \\ \vdots \\ \alpha_m \end{bmatrix}, \qquad \begin{bmatrix} \tilde{\beta}_1 \\ \tilde{\beta}_2 \\ \vdots \\ \tilde{\beta}_n \end{bmatrix} = \boldsymbol{T}_4^T \begin{bmatrix} \beta_1 \\ \beta_2 \\ \vdots \\ \beta_n \end{bmatrix}$$
$$\begin{bmatrix} \tilde{r}_{11} & \tilde{r}_{12} & \cdots & \tilde{r}_{1n} \\ \tilde{r}_{21} & \tilde{r}_{22} & \cdots & \tilde{r}_{2n} \\ \vdots & \vdots & \ddots & \vdots \\ \tilde{r}_{m1} & \tilde{r}_{m2} & \cdots & \tilde{r}_{mn} \end{bmatrix} = \boldsymbol{T}_1^{-1} \begin{bmatrix} r_{11} & r_{12} & \cdots & r_{1n} \\ r_{21} & r_{22} & \cdots & r_{2n} \\ \vdots & \vdots & \ddots & \vdots \\ r_{m1} & r_{m2} & \cdots & r_{mn} \end{bmatrix} \boldsymbol{T}_4$$
$$\begin{bmatrix} \tilde{r}_{01} & \tilde{r}_{02} & \cdots & \tilde{r}_{0n} \end{bmatrix} = \begin{bmatrix} r_{01} & r_{02} & \cdots & r_{0n} \end{bmatrix} \boldsymbol{T}_4$$
$$\begin{bmatrix} \tilde{r}_{10} & \tilde{r}_{20} & \cdots & \tilde{r}_{m0} \end{bmatrix}^T = \boldsymbol{T}_1^{-1} \begin{bmatrix} r_{10} & r_{20} & \cdots & r_{m0} \end{bmatrix}^T \tag{19}$$

2.4 l_2-Scaling Constraints

The horizontal and vertical controllability Grammians $\tilde{\boldsymbol{K}}^h$

and $\tilde{\boldsymbol{K}}^v$ of the local state-space model in (16) play an important role in the dynamic-range scaling of the local state vectors $\boldsymbol{x}^h(i,j)$ and $\boldsymbol{x}^v(i,j)$ in (14). The Grammians $\tilde{\boldsymbol{K}}^h$ and $\tilde{\boldsymbol{K}}^v$ can be obtained by solving the Lyapunov equations [19]

$$\begin{aligned}\tilde{\boldsymbol{K}}^h &= \tilde{\boldsymbol{A}}_1\tilde{\boldsymbol{K}}^h\tilde{\boldsymbol{A}}_1^T + \tilde{\boldsymbol{A}}_2\tilde{\boldsymbol{K}}^v\tilde{\boldsymbol{A}}_2^T + \tilde{\boldsymbol{b}}_1\tilde{\boldsymbol{b}}_1^T\\ \tilde{\boldsymbol{K}}^v &= \tilde{\boldsymbol{A}}_4\tilde{\boldsymbol{K}}^v\tilde{\boldsymbol{A}}_4^T + \tilde{\boldsymbol{b}}_2\tilde{\boldsymbol{b}}_2^T\end{aligned} \tag{20}$$

respectively. With an equivalent realization specified in (18), the horizontal and vertical controllability Grammians $\boldsymbol{K}^h$ and $\boldsymbol{K}^v$ of the local state-space model in (14) assumes the form

$$\boldsymbol{K}^h = \boldsymbol{T}_1\tilde{\boldsymbol{K}}^h\boldsymbol{T}_1^T, \qquad \boldsymbol{K}^v = \boldsymbol{T}_4\tilde{\boldsymbol{K}}^v\boldsymbol{T}_4^T \tag{21}$$

where

$$\boldsymbol{T}_1 = \mathrm{diag}\{\bar{t}_1,\bar{t}_2,\cdots,\bar{t}_m\}, \qquad \boldsymbol{T}_4 = \mathrm{diag}\{\hat{t}_1,\hat{t}_2,\cdots,\hat{t}_n\}$$

If l_2-scaling constraints are imposed on the horizontal and vertical state vectors $\boldsymbol{x}^h(i,j)$ and $\boldsymbol{x}^v(i,j)$ in (14), the horizontal and vertical controllability Grammians $\boldsymbol{K}^h$ and $\boldsymbol{K}^v$ of the local state-space model in (14) are subject to the constraints

$$\begin{aligned}&\bar{\boldsymbol{e}}_k^T\boldsymbol{K}^h\bar{\boldsymbol{e}}_k = \bar{\boldsymbol{e}}_k^T\boldsymbol{T}_1\tilde{\boldsymbol{K}}^h\boldsymbol{T}_1^T\bar{\boldsymbol{e}}_k = \bar{t}_k^2\bar{\boldsymbol{e}}_k^T\tilde{\boldsymbol{K}}^h\bar{\boldsymbol{e}}_k = 1\\ &\qquad \text{for } k = 1,2,\cdots,m\\ &\hat{\boldsymbol{e}}_l^T\boldsymbol{K}^v\hat{\boldsymbol{e}}_l = \hat{\boldsymbol{e}}_l^T\boldsymbol{T}_4\tilde{\boldsymbol{K}}^v\boldsymbol{T}_4^T\hat{\boldsymbol{e}}_l = \hat{t}_l^2\hat{\boldsymbol{e}}_l^T\tilde{\boldsymbol{K}}^v\hat{\boldsymbol{e}}_l = 1\\ &\qquad \text{for } l = 1,2,\cdots,n\end{aligned} \tag{22}$$

where $\bar{\boldsymbol{e}}_k$ ($\hat{\boldsymbol{e}}_l$) indicates the kth (lth) column of $m\times m$ ($n\times n$) identity matrix $\boldsymbol{I}_m$ ($\boldsymbol{I}_n$). By noting that $\bar{t}_k = (\bar{\Delta}_1\bar{\Delta}_2\cdots\bar{\Delta}_k)^{-1}$ for $k = 1,2,\cdots,m$ and $\hat{t}_l = \hat{\Delta}_1\hat{\Delta}_2\cdots\hat{\Delta}_l$ for $l = 1,2,\cdots,n$, we obtain

$$\begin{aligned}&\bar{\Delta}_1 = \sqrt{\bar{\boldsymbol{e}}_1^T\tilde{\boldsymbol{K}}^h\bar{\boldsymbol{e}}_1},\quad \bar{\Delta}_2 = \sqrt{\frac{\bar{\boldsymbol{e}}_2^T\tilde{\boldsymbol{K}}^h\bar{\boldsymbol{e}}_2}{\bar{\boldsymbol{e}}_1^T\tilde{\boldsymbol{K}}^h\bar{\boldsymbol{e}}_1}},\quad \cdots,\\ &\bar{\Delta}_m = \sqrt{\frac{\bar{\boldsymbol{e}}_m^T\tilde{\boldsymbol{K}}^h\bar{\boldsymbol{e}}_m}{\bar{\boldsymbol{e}}_{m-1}^T\tilde{\boldsymbol{K}}^h\bar{\boldsymbol{e}}_{m-1}}},\quad \hat{\Delta}_1 = \frac{1}{\sqrt{\hat{\boldsymbol{e}}_1^T\tilde{\boldsymbol{K}}^v\hat{\boldsymbol{e}}_1}}\\ &\hat{\Delta}_2 = \sqrt{\frac{\hat{\boldsymbol{e}}_1^T\tilde{\boldsymbol{K}}^v\hat{\boldsymbol{e}}_1}{\hat{\boldsymbol{e}}_2^T\tilde{\boldsymbol{K}}^v\hat{\boldsymbol{e}}_2}},\quad \cdots,\quad \hat{\Delta}_n = \sqrt{\frac{\hat{\boldsymbol{e}}_{n-1}^T\tilde{\boldsymbol{K}}^v\hat{\boldsymbol{e}}_{n-1}}{\hat{\boldsymbol{e}}_n^T\tilde{\boldsymbol{K}}^v\hat{\boldsymbol{e}}_n}}\end{aligned} \tag{23}$$

where parameters $\{\bar{\Delta}_k\}$ and $\{\hat{\Delta}_l\}$ are called the *coupling coefficients* [13]. It is clear from the above analysis that overflow oscillations can be avoided if these coupling coefficients are used to scale the state variables.

3. Analysis and Minimization of Roundoff Noise

3.1 Roundoff Noise of State-Space Realization in (14)

It is known that the roundoff noise measure due to product quantization associated with the coefficient matrices $\boldsymbol{A}_1$, $\boldsymbol{A}_2$, $\boldsymbol{A}_4$, $\boldsymbol{b}_1$, $\boldsymbol{b}_2$, $\boldsymbol{c}_1$, $\boldsymbol{c}_2$ and d in (14) can be expressed as [19]

$$J_{S\rho} = \mathrm{tr}[\boldsymbol{Q}^h\boldsymbol{W}^h] + \mathrm{tr}[\boldsymbol{Q}^v\boldsymbol{W}^v] + q \tag{24a}$$

where $\boldsymbol{W}^h$ and $\boldsymbol{W}^v$ are the horizontal and vertical observability Grammians of the local state-space model in (14), which can be obtained by solving the Lyapunov equations [19]

$$\begin{aligned}\boldsymbol{W}^h &= \boldsymbol{A}_1^T\boldsymbol{W}^h\boldsymbol{A}_1 + \boldsymbol{c}_1^T\boldsymbol{c}_1\\ \boldsymbol{W}^v &= \boldsymbol{A}_4^T\boldsymbol{W}^v\boldsymbol{A}_4 + \boldsymbol{A}_2^T\boldsymbol{W}^h\boldsymbol{A}_2 + \boldsymbol{c}_2^T\boldsymbol{c}_2\end{aligned} \tag{24b}$$

respectively, $\boldsymbol{Q}^h$ ($\boldsymbol{Q}^v$) is a diagonal matrix whose kth (lth) diagonal element q_k^h (q_l^v) is the number of coefficients in the kth (lth) row of $\boldsymbol{A}_1$, $\boldsymbol{A}_2$ and $\boldsymbol{b}_1$ ($\boldsymbol{A}_4$ and $\boldsymbol{b}_2$) that are neither 0 nor ±1, and q is the number of neither 0 nor ±1 constant in $\boldsymbol{c}_1$, $\boldsymbol{c}_2$ and d.

If (24a) is applied to the state-space realization in (14), the corresponding roundoff noise measure $J_{S\rho}$ is characterized by

$$\begin{aligned}&q_1^h = n+3, \quad q_k^h = n+3+\psi(\bar{\gamma}_k) \ \text{ for } \ k = 2,\cdots,m-1\\ &q_m^h = n+2+\psi(\bar{\gamma}_m), \qquad q = n+2\\ &q_1^v = n+1, \quad q_l^v = 1+\psi(\hat{\gamma}_l) \ \text{ for } \ l = 2,3,\cdots,n\end{aligned} \tag{25}$$

where function

$$\psi(\gamma) = \begin{cases} 1 & \text{for} \quad \gamma \neq 0, \pm1\\ 0 & \text{for} \quad \gamma = 0, \pm1\end{cases}$$

is introduced due to a special choice of sets $\{\bar{\gamma}_k | k = 1,2,\cdots,m\}$ and $\{\hat{\gamma}_l | l = 1,2,\cdots,n\}$.

By substituting (25) into (24a), we obtain

$$\begin{aligned}J_{S\rho} &= (n+3)\mathrm{tr}[\boldsymbol{W}^h] - \bar{\boldsymbol{e}}_m^T\boldsymbol{W}^h\bar{\boldsymbol{e}}_m\\ &\quad + \sum_{k=2}^{m}\psi(\bar{\gamma}_k)\bar{\boldsymbol{e}}_k^T\boldsymbol{W}^h\bar{\boldsymbol{e}}_k + n\hat{\boldsymbol{e}}_1^T\boldsymbol{W}^v\hat{\boldsymbol{e}}_1\\ &\quad + \mathrm{tr}[\boldsymbol{W}^v] + \sum_{l=2}^{n}\psi(\hat{\gamma}_l)\hat{\boldsymbol{e}}_l^T\boldsymbol{W}^v\hat{\boldsymbol{e}}_l + n + 2\end{aligned} \tag{26}$$

3.2 Roundoff Noise of Filter Structure in (10)

The roundoff noise measure for the filter structure in (10) can be written as

$$\begin{aligned}J_\rho &= (n+3)\,\mathrm{tr}[\boldsymbol{W}^h] - \bar{\boldsymbol{e}}_m^T\boldsymbol{W}^h\bar{\boldsymbol{e}}_m + \mathrm{tr}[\bar{\boldsymbol{\Psi}}\boldsymbol{W}^h]\\ &\quad + (n+2)(\boldsymbol{\alpha}^T\boldsymbol{W}^h\boldsymbol{\alpha}+1) + \mathrm{tr}[\boldsymbol{W}^v] + \mathrm{tr}[\hat{\boldsymbol{\Psi}}\boldsymbol{W}^v]\\ &\quad + n(\boldsymbol{b}_1^T\boldsymbol{W}^h\boldsymbol{b}_1 + \boldsymbol{b}_2^T\boldsymbol{W}^v\boldsymbol{b}_2 + d^2)\end{aligned} \tag{27}$$

where

$$\begin{aligned}\bar{\boldsymbol{\Psi}} &= \mathrm{diag}\{\psi(\bar{\gamma}_1),\psi(\bar{\gamma}_2),\cdots,\psi(\bar{\gamma}_m)\}\\ \hat{\boldsymbol{\Psi}} &= \mathrm{diag}\{\psi(\hat{\gamma}_1),\psi(\hat{\gamma}_2),\cdots,\psi(\hat{\gamma}_n)\}\end{aligned}$$

The reader is referred to the Appendix for the details of deriving (27).

It is interesting to note that the difference

$$\begin{aligned} J_\rho - J_{S\rho} = \psi(\overline{\gamma}_1)\overline{\boldsymbol{e}}_1^T \boldsymbol{W}^h \overline{\boldsymbol{e}}_1 + \psi(\hat{\gamma}_1)\hat{\boldsymbol{e}}_1^T \boldsymbol{W}^v \hat{\boldsymbol{e}}_1 \\ + (n+2)\boldsymbol{\alpha}^T \boldsymbol{W}^h \boldsymbol{\alpha} \\ + n\left[\boldsymbol{b}_1^T \boldsymbol{W}^h \boldsymbol{b}_1 + (\hat{\Delta}_1^2 - 1)\hat{\boldsymbol{e}}_1^T \boldsymbol{W}^v \hat{\boldsymbol{e}}_1 + d^2\right] \end{aligned} \tag{28}$$

is due to the different number of coefficients between the filter structure in (10) (see Fig. 2) and its state-space realization in (14).

3.3 Computation of Roundoff Noise

Given $\{\overline{\gamma}_k \mid k = 1, 2, \cdots, m\}$ and $\{\hat{\gamma}_l \mid l = 1, 2, \cdots, n\}$, a concrete procedure for evaluating the roundoff noise for the generalized direct-form II state-space realization and filter structure can be summarized as follows:
Step 1. Calculate $\boldsymbol{P}_1$ and $\boldsymbol{P}_2$ from (7) or (8) subject to $\overline{\Delta}_k = 1$ for $k = 1, 2, \cdots, m$ and $\hat{\Delta}_l = 1$ for $l = 1, 2, \cdots, n$.
Step 2. Compute $\tilde{\boldsymbol{\alpha}} = [\tilde{\alpha}_1, \tilde{\alpha}_2, \cdots, \tilde{\alpha}_m]^T$, $\tilde{\boldsymbol{\beta}} = [\tilde{\beta}_1, \tilde{\beta}_2, \cdots, \tilde{\beta}_n]^T$ and $\{\tilde{r}_{kl} \mid k = 0, 1, \cdots, m;\ l = 0, 1, \cdots, n\}$ using

$$\begin{aligned} \begin{bmatrix} 1 & \tilde{\alpha}_1 & \cdots & \tilde{\alpha}_m \end{bmatrix} \boldsymbol{P}_1 &= \begin{bmatrix} 1 & a_1 & \cdots & a_m \end{bmatrix} \\ \begin{bmatrix} 1 & \tilde{\beta}_1 & \cdots & \tilde{\beta}_n \end{bmatrix} \boldsymbol{P}_2 &= \begin{bmatrix} 1 & b_1 & \cdots & b_n \end{bmatrix} \\ \boldsymbol{P}_1^T \begin{bmatrix} \tilde{r}_{00} & \cdots & \tilde{r}_{0n} \\ \vdots & \ddots & \vdots \\ \tilde{r}_{m0} & \cdots & \tilde{r}_{mn} \end{bmatrix} \boldsymbol{P}_2 &= \begin{bmatrix} c_{00} & \cdots & c_{0n} \\ \vdots & \ddots & \vdots \\ c_{m0} & \cdots & c_{mn} \end{bmatrix} \end{aligned} \tag{29}$$

from given $\{a_k | k = 1, 2, \cdots, m\}$, $\{b_l | l = 1, 2, \cdots, n\}$ and $\{c_{kl} \mid k = 0, 1, \cdots, m;\ l = 0, 1, \cdots, n\}$.
Step 3. Construct the corresponding state-space realization in (16).
Step 4. Obtain the horizontal and vertical controllability Grammians $\tilde{\boldsymbol{K}}^h$ and $\tilde{\boldsymbol{K}}^v$ by solving the Lyapunov equations in (20).
Step 5. Compute the l_2-scaling factors $\overline{\Delta}_k$ for $k = 1, 2, \cdots, m$ and $\hat{\Delta}_l$ for $l = 1, 2, \cdots, n$ via (23).
Step 6. Find $\boldsymbol{\alpha} = [\alpha_1, \alpha_2, \cdots, \alpha_m]^T$, $\boldsymbol{\beta} = [\beta_1, \beta_2, \cdots, \beta_n]^T$ and $\{r_{kl} \mid k = 0, 1, \cdots, m;\ l = 0, 1, \cdots, n\}$ that are l_2-scaled by using (19).
Step 7. Construct the l_2-scaled state-space realization in (14).
Step 8. Obtain the horizontal and vertical observability Grammians $\boldsymbol{W}^h$ and $\boldsymbol{W}^v$ by solving the Lyapunov equations in (24b).
Step 9. Compute the roundoff noise measures $J_{S\rho}$ and J_ρ via (26) and (27), respectively.

3.4 Choice of Parameters $\{\overline{\gamma}_i\}$ and $\{\hat{\gamma}_l\}$

In this section we address an issue on the performance of generalized direct-form II realization and structure for a 2-D separable-denominator digital filter from the viewpoint of roundoff noise measures. Each performance measure is a function of parameters $\overline{\gamma}_k$ for $k = 1, 2, \cdots, m$ and $\hat{\gamma}_l$ for $l = 1, 2, \cdots, n$. In theory, these parameters can be chosen from a set of real numbers. However, our attention is confined to fix-point implementation where the FWL effects are more serious, and therefore we assume in the sequel that $|\overline{\gamma}_k| \le 1$ for $k = 1, 2, \cdots, m$ and $|\hat{\gamma}_l| \le 1$ for $l = 1, 2, \cdots, n$.

For a fixed-point implementation of B_c bits, every $\overline{\gamma}_i$ and $\hat{\gamma}_l$ must be truncated or rounded into a B_γ-bit number ($B_\gamma \le B_c$) of the form

$$v = \pm \sum_{p=1}^{B_\gamma} b_p 2^{-p} \text{ with } b_p = 0, 1 \ \ \forall\, p \tag{30}$$

unless $v = \pm 1$. Hence $\overline{\gamma}_i$ and $\hat{\gamma}_l$ should take values within a *discrete space* defined by

$$S_\gamma = \{-1, 1\} \cup \left\{ \pm \sum_{p=1}^{B_\gamma} b_p 2^{-p},\ \ b_p = 0, 1 \ \ \forall\, p \right\} \tag{31}$$

which contains $(2^{B_\gamma+1} + 1)$ elements. Hereafter, we assume that all parameters $\overline{\gamma}_k$ for $k = 1, 2, \cdots, m$ and $\hat{\gamma}_l$ for $l = 1, 2, \cdots, n$ belong to S_γ, *i.e.*, $\overline{\gamma}_k \in S_\gamma \ \forall\, k$ and $\hat{\gamma}_l \in S_\gamma \ \forall\, l$. Hence, these parameters cause the roundoff noise unless they are trivial.

3.5 Search of Optimal Vector $\boldsymbol{\gamma} = [\overline{\gamma}_1, \cdots, \overline{\gamma}_m, \hat{\gamma}_1, \cdots, \hat{\gamma}_n]^T$

Let $\tilde{S}_{\boldsymbol{\gamma}} \in \boldsymbol{R}^{(m+n)\times 1}$ be the space in which $\boldsymbol{\gamma}$ resides, i.e.,

$$\tilde{S}_{\boldsymbol{\gamma}} = \{\boldsymbol{\gamma} \mid \gamma_k \in S_\gamma \ \ \forall\, k\} \tag{32}$$

where $\boldsymbol{\gamma} = [\gamma_1, \gamma_2, \cdots, \gamma_{m+n}]^T$. It is obvious that $J_{S\rho}$ in (26) and J_ρ in (27) are functions of vector $\boldsymbol{\gamma}$ because the Grammians depend on $\boldsymbol{\gamma}$. Consequently, the problem of minimizing $J_{S\rho}$ or J_ρ with respect to vector $\boldsymbol{\gamma}$ subject to the l_2-scaling constraints in (22) can be described as

$$\begin{aligned} \boldsymbol{\gamma}(J_{S\rho}^{opt}) &= \arg \min_{\boldsymbol{\gamma} \in \tilde{S}_{\boldsymbol{\gamma}}} J_{S\rho} \ \text{ subject to (22)} \\ \boldsymbol{\gamma}(J_\rho^{opt}) &= \arg \min_{\boldsymbol{\gamma} \in \tilde{S}_{\boldsymbol{\gamma}}} J_\rho \ \text{ subject to (22)} \end{aligned} \tag{33}$$

Since $J_{S\rho}$ and J_ρ are highly nonlinear and non-convex functions with respect to $\boldsymbol{\gamma}$, finding the solutions of the problems in (33) is rather challenging. However, the problems can easily be solved using exhaustive search since the space $\overline{S}_{\boldsymbol{\gamma}}$ includes $(2^{B_\gamma+1} + 1)^{m+n}$ elements where $m + n$ is the filter order, and B_γ is the number of bits for implementing $\{\overline{\gamma}_i\}$ and $\{\hat{\gamma}_l\}$ with 4 to 8 bits typically. Hence by repeating a search procedure a finite number of times, one can eventually find the optimal solution $\boldsymbol{\gamma}(J_{S\rho}^{opt})$ or $\boldsymbol{\gamma}(J_\rho^{opt})$.

4. Numerical Experiments

Consider a 2-D stable separable-denominator digital filter in (1) of order $(m, n) = (3, 3)$ specified by

$$\begin{aligned} \begin{bmatrix} a_1 & a_2 & a_3 \end{bmatrix} &= \begin{bmatrix} -2.173645 & 1.836929 & -0.599655 \end{bmatrix} \\ \begin{bmatrix} b_1 & b_2 & b_3 \end{bmatrix} &= \begin{bmatrix} -2.280029 & 1.887939 & -0.564961 \end{bmatrix} \end{aligned}$$

$$\begin{bmatrix} c_{00} & \cdots & c_{03} \\ \vdots & \ddots & \vdots \\ c_{30} & \cdots & c_{33} \end{bmatrix} = 10^{-2} \cdot \begin{bmatrix} 1.942100 & -2.772444 & 1.146750 & -0.008675 \\ 0.483864 & 1.754489 & -5.026688 & 3.306088 \\ -0.432752 & -0.884715 & 9.625968 & -8.380145 \\ -0.013845 & 0.797858 & -5.292746 & 6.260656 \end{bmatrix}$$

As the first scenario, if $\overline{\Delta}_k = \hat{\Delta}_l = 1$ and $\overline{\gamma}_k = \hat{\gamma}_l = 1$ for $k, l = 1, 2, 3$ then the filter was realized with either (7) or (8) and (29) by the local state-space model in (16) as

$$\tilde{A}_1 = \begin{bmatrix} -0.826355 & 1 & 0 \\ -0.489639 & 0 & 1 \\ -0.063629 & 0 & 0 \end{bmatrix} + \mathrm{diag}\{1,\ 1,\ 1\}$$

$$\tilde{A}_2 = 10^{-2} \begin{bmatrix} 6.456400 & 1.495421 & 0.984562 \\ 8.000178 & 8.237299 & 1.504009 \\ 3.302859 & 3.482411 & 2.406478 \end{bmatrix}$$

$$\tilde{A}_4 = \begin{bmatrix} -0.719971 & 1 & 0 \\ -0.327881 & 0 & 1 \\ -0.042949 & 0 & 0 \end{bmatrix}^T + \mathrm{diag}\{1,\ 1,\ 1\}$$

$$\tilde{b}_1 = 10^{-2} \begin{bmatrix} 4.705300 & 5.410348 & 1.855793 \end{bmatrix}^T$$

$$\tilde{b}_2 = \begin{bmatrix} 1 & 0 & 0 \end{bmatrix}^T, \qquad \tilde{c}_1 = \begin{bmatrix} 1 & 0 & 0 \end{bmatrix}$$

$$\tilde{c}_2 = 10^{-2} \begin{bmatrix} 1.655600 & 0.791384 & 0.224319 \end{bmatrix}$$

$$\tilde{d} = 1.942100 \times 10^{-2}$$

By solving the Lyapunov equations in (20), we got

$$\tilde{K}^h = 10^{-1} \begin{bmatrix} 9.846378 & 7.194732 & 2.749809 \\ 7.194732 & 6.959876 & 2.754669 \\ 2.749809 & 2.754669 & 1.459376 \end{bmatrix}$$

$$\tilde{K}^v = \begin{bmatrix} 2.269178 & -1.134589 & -5.604971 \\ -1.134589 & 6.739560 & -3.369780 \\ -5.604971 & -3.369780 & 64.205001 \end{bmatrix}$$

From (23) and (19), it was derived that

$$\begin{bmatrix} \overline{\Delta}_1 & \overline{\Delta}_2 & \overline{\Delta}_3 \end{bmatrix} = \begin{bmatrix} 0.992289 & 0.840742 & 0.457913 \end{bmatrix}$$

$$\begin{bmatrix} \hat{\Delta}_1 & \hat{\Delta}_2 & \hat{\Delta}_3 \end{bmatrix} = \begin{bmatrix} 0.663843 & 0.580255 & 0.323990 \end{bmatrix}$$

$$T_1^{-1} = \mathrm{diag}\{0.992289,\ 0.834259,\ 0.382018\}$$

$$T_4 = \mathrm{diag}\{0.663843,\ 0.385198,\ 0.124800\}$$

Then (18) was used to obtain

$$A_1 = 10^{-1} \begin{bmatrix} -8.263550 & 8.407415 & 0 \\ -5.823895 & 0 & 4.579129 \\ -1.652760 & 0 & 0 \end{bmatrix} + \mathrm{diag}\{1,\ 1,\ 1\}$$

$$A_2 = 10^{-1} \begin{bmatrix} 0.980136 & 0.391238 & 0.795041 \\ 1.444552 & 2.563302 & 1.444555 \\ 1.302389 & 2.366531 & 5.047574 \end{bmatrix}$$

$$A_4 = 10^{-1} \begin{bmatrix} -7.199710 & -5.650641 & -2.284563 \\ 5.802545 & 0 & 0 \\ 0 & 3.239898 & 0 \end{bmatrix} + \mathrm{diag}\{1,\ 1,\ 1\}$$

$$b_1 = 10^{-2} \begin{bmatrix} 4.741864 \\ 6.485216 \\ 4.857871 \end{bmatrix}, \quad b_2 = 10^{-1} \begin{bmatrix} 6.638435 \\ 0 \\ 0 \end{bmatrix}$$

$$c_1 = 10^{-1} \begin{bmatrix} 9.922892 & 0 & 0 \end{bmatrix}$$

$$c_2 = 10^{-2} \begin{bmatrix} 2.493961 & 2.054485 & 1.797427 \end{bmatrix}$$

$$d = \tilde{d} = 1.942100 \times 10^{-2}$$

By solving the Lyapunov equations in (24b), we had

$$W^h = \begin{bmatrix} 2.588217 & -1.088011 & -1.523551 \\ -1.088011 & 3.712020 & -0.849891 \\ -1.523551 & -0.849891 & 4.488465 \end{bmatrix}$$

$$W^v = \begin{bmatrix} 2.206126 & 2.506623 & 2.367291 \\ 2.506623 & 3.389244 & 3.415169 \\ 2.367291 & 3.415169 & 4.150797 \end{bmatrix}$$

In this case, we derived from (26) and (31) that

$$J_{S\rho} = 81.608287, \qquad J_\rho = 85.675434$$

As the second scenario, if the procedure stated in Sect. 3.3 was repeated with respect to the free parameters $\overline{\gamma}_k$ for $k = 1, 2, 3$ and $\hat{\gamma}_l$ for $l = 1, 2, 3$ over a set with finite number of candidate elements, we arrived at

$$\gamma(J_{S\rho}^{opt}) = [0.250,\ 0.625,\ 0.750,\ -0.750,\ 0.750,\ 0.750]^T$$

Then, in case $\overline{\Delta}_k = \hat{\Delta}_l = 1$ for $k, l = 1, 2, 3$, the filter was realized with either (7) or (8) and (29) by the local state-space model in (16) as

$$\tilde{A}_1 = \begin{bmatrix} 0.548645 & 1 & 0 \\ -0.270042 & 0 & 1 \\ 0.022759 & 0 & 0 \end{bmatrix} + \begin{bmatrix} 0.250 & 0 & 0 \\ 0 & 0.625 & 0 \\ 0 & 0 & 0.750 \end{bmatrix}$$

$$\tilde{A}_2 = 10^{-2} \begin{bmatrix} 6.456400 & -1.732779 & 1.014232 \\ 3.964928 & 5.320197 & -0.689200 \\ 1.706339 & 0.663380 & 1.819520 \end{bmatrix}$$

$$\tilde{A}_4 = \begin{bmatrix} 1.530029 & 1 & 0 \\ -0.155396 & 0 & 1 \\ 0.009648 & 0 & 0 \end{bmatrix}^T + \begin{bmatrix} -0.750 & 0 & 0 \\ 0 & 0.750 & 0 \\ 0 & 0 & 0.750 \end{bmatrix}$$

$$\tilde{b}_1 = 10^{-2} \begin{bmatrix} 4.705300 & 2.469536 & 0.797288 \end{bmatrix}^T$$

$$\tilde{b}_2 = \begin{bmatrix} 1 & 0 & 0 \end{bmatrix}^T, \qquad \tilde{c}_1 = \begin{bmatrix} 1 & 0 & 0 \end{bmatrix}$$

$$\tilde{c}_2 = 10^{-2} \begin{bmatrix} 1.655600 & -0.036416 & 0.129948 \end{bmatrix}$$

By solving the Lyapunov equations in (20), we got

$$\tilde{K}^h = 10^{-1} \begin{bmatrix} 9.846378 & 1.040745 & 1.566525 \\ 1.040745 & 1.812703 & 0.485292 \\ 1.566525 & 0.485292 & 0.674387 \end{bmatrix}$$

$$\tilde{K}^v = \begin{bmatrix} 2.159047 & 1.205318 & -3.277048 \\ 1.205318 & 9.067483 & 12.681470 \\ -3.277048 & 12.681470 & 64.205001 \end{bmatrix}$$

From (23) and (19), it was derived that

$$\begin{bmatrix} \overline{\Delta}_1 & \overline{\Delta}_2 & \overline{\Delta}_3 \end{bmatrix} = \begin{bmatrix} 0.992289 & 0.429067 & 0.609946 \end{bmatrix}$$

$$\begin{bmatrix} \hat{\Delta}_1 & \hat{\Delta}_2 & \hat{\Delta}_3 \end{bmatrix} = \begin{bmatrix} 0.680564 & 0.487964 & 0.375802 \end{bmatrix}$$

$$\boldsymbol{T}_1^{-1} = \mathrm{diag}\{0.992289,\ 0.425759,\ 0.259690\}$$

$$\boldsymbol{T}_4 = \mathrm{diag}\{0.680564,\ 0.332091,\ 0.124800\}$$

Then (18) was used to obtain

$$\boldsymbol{A}_1 = 10^{-1}\begin{bmatrix} 5.486450 & 4.290670 & 0 \\ -6.293705 & 0 & 6.099459 \\ 0.869618 & 0 & 0 \end{bmatrix} + \mathrm{diag}\{0.250,\ 0.625,\ 0.750\}$$

$$\boldsymbol{A}_2 = 10^{-1}\begin{bmatrix} 0.956056 & -0.525834 & 0.818999 \\ 1.368368 & 3.762770 & -1.297080 \\ 0.965477 & 0.769221 & 5.614182 \end{bmatrix}$$

$$\boldsymbol{A}_4 = \begin{bmatrix} 1.530029 & -0.318457 & 0.052613 \\ 0.487964 & 0 & 0 \\ 0 & 0.375802 & 0 \end{bmatrix} + \mathrm{diag}\{-0.750,\ 0.750,\ 0.750\}$$

$$\boldsymbol{b}_1 = 10^{-2}\begin{bmatrix} 4.741864 \\ 5.800320 \\ 3.070155 \end{bmatrix}, \quad \boldsymbol{b}_2 = \begin{bmatrix} 0.680564 \\ 0 \\ 0 \end{bmatrix}$$

$$\boldsymbol{c}_1 = 10^{-1}\begin{bmatrix} 9.922892 & 0 & 0 \end{bmatrix}$$

$$\boldsymbol{c}_2 = 10^{-2}\begin{bmatrix} 2.432688 & -0.109657 & 1.041251 \end{bmatrix}$$

By solving the Lyapunov equations in (24b), we had

$$\boldsymbol{W}^h = \begin{bmatrix} 2.238400 & 0.451409 & -0.722164 \\ 0.451409 & 1.073546 & 0.555289 \\ -0.722164 & 0.555289 & 2.074149 \end{bmatrix}$$

$$\boldsymbol{W}^v = \begin{bmatrix} 2.099055 & 0.685216 & 1.137881 \\ 0.685216 & 0.951810 & 0.728505 \\ 1.137881 & 0.728505 & 1.430111 \end{bmatrix}$$

In this case, we derived from (26) and (27) that

$$J_{S\rho} = 51.550177, \qquad J_\rho = 54.240666$$

respectively.

If the procedure stated in Sect. 3.3 was repeated about the free parameters $\overline{\gamma}_k$ and $\hat{\gamma}_l$ for $k, l = 1, 2, 3$ over a set with finite number of candidate elements, we arrived at

$$\boldsymbol{\gamma}(J_\rho^{opt}) = [1.000,\ 0.625,\ 0.750,\ 0.000,\ 1.000,\ 0.625]^T$$

In this case, it was derived from (26) and (27) that

$$J_{S\rho} = 54.240666, \qquad J_\rho = 51.293498$$

The results obtained by this example are summarized in Table 1 in comparison with two cases of $\boldsymbol{\gamma}_z = [0, 0, \cdots, 0]^T$ and $\boldsymbol{\gamma}_\delta = [1, 1, \cdots, 1]^T$. Moreover, the proposed techniques are compared with the existing ones in Table 2. These results have clearly demonstrated an important role that parameters $\overline{\gamma}_k$'s and $\hat{\gamma}_l$'s can play, especially in the case when they are optimized by using the present techniques.

From Table 2, it is observed that the roundoff noise $J_\rho^{opt} = 51.2935$ is secondly minimum among them with the least filter implementation cost where there are at most $4(m+n)+mn+1$ nontrivial coefficients such that the implementation cost can be reduced for 2-D separable-denominator filters with $m, n > 1$. The method in [19] yields the largest roundoff noise among them and its filter implementation is costly where $m^2+mn+n^2+2(m+n)+1$ nontrivial coefficients exist. The one in [21] produces the minimum roundoff noise among them. However, its filter implementation is still costly as in [19]. Moreover, $J_{S\rho}^{opt} = 51.5502$ is located between $J_\rho^{opt} = 51.2935$ and $J_{min} = 51.6701$ in [19] which requires the secondly least filter implementation cost where at most $4(m+n)+mn-1$ nontrivial coefficients exist. Note that unlike [19], [20] and this paper, quantizations were performed *before* multiplications in [22], [23]. Hence, fair comparison with the techniques in [22], [23] might be impossible.

Table 1 Performance comparison among various $\boldsymbol{\gamma}$.

	$\boldsymbol{\gamma}_z$	$\boldsymbol{\gamma}_\delta$	$\boldsymbol{\gamma}(J_{S\rho}^{opt})$	$\boldsymbol{\gamma}(J_\rho^{opt})$
$J_{S\rho}$	958.0212	81.6083	51.5502	54.2407
J_ρ	922.4951	85.6754	55.9660	51.2935

Table 2 Performance comparison among techniques.

	Ref. [19]	Ref. [21]	$J_{S\rho}^{opt}$	J_ρ^{opt}
Minimized Roundoff Noise	51.6701	36.8123	51.5502	51.2935
Nontrivial Coefficients	40	40	32	31

5. Conclusion

Based on the concept of polynomial operators, generalized direct-form II structure and state-space realization of 2-D separable-denominator digital filters have been explored. Then an l_2-scaling method has been introduced by employing different coupling coefficients at different branch nodes to avoid overflow. Expressions of evaluating the roundoff noise for generalized direct form II structure and its state-space realization have been derived and investigated. In addition, the roundoff noise measures have been minimized with respect to the free parameters subject to l_2-scaling constraints through exhaustive search in a finite element space. The results of a numerical example have demonstrated the validity and effectiveness of the proposed techniques.

References

[1] P.K. Rajan and M.N.S. Swamy, "Design of separable denominator

2-dimensional digital filters possessing real circularly symmetric frequency responses," Proc. Inst. Elect. Eng. G, vol.129, no.5, pp.235–240, Oct. 1982.
[2] M.N.S. Swamy and P.K. Rajan, "Symmetry in 2-D filters and its application," Multidimensional Systems: Techniques and Applications, ed. S. Tzafestas, ch. 9, Marcel Dekkar, New York, 1986.
[3] H.K. Kwan and C.L. Chan, "Design of linear phase circularly symmetric two-dimensional recursive digital filters," IEEE Trans. Circuits Syst., vol.36, no.7, pp.1023–1029, July 1989.
[4] C. Xiao and P. Agathoklis, "Design and implementation of approximately linear phase two-dimensional IIR filters," IEEE Trans. Circuits Syst. II, Analog Digit. Signal Process., vol.45, no.9, pp.1279–1288, Sept. 1998.
[5] H.C. Reddy, I.-H. Khoo, and P.K. Rajan, "2-D symmetry: Theory and filter design applications," IEEE Circuits Syst. Mag., vol.3, no.3, pp.4–33, 3rd Q., 2003.
[6] H.C. Reddy, I.-H. Khoo, and P.K. Rajan, "Application of symmetry: 2-D polynomials, Fourier transform, and filter design," The Circuits and Filters Handbook, ed. W.K. Chen, 3rd ed., CRC, Boca Raton, FL, 2009.
[7] P.-Y. Chen, L.-D. Van, I.-H. Khoo, H.C. Reddy and C.-T. Lin, "Power-efficient and cost-effective 2-D symmetry filter architectures," IEEE Trans. Circuits Syst. I, Reg. Papers, vol.58, no.1, pp.112–125, Jan. 2011.
[8] L.-D. Van, I.-H. Khoo, P.-Y. Chen, and H.C. Reddy, "Symmetry incorporated cost-effective architectures for two-dimensional digital filters," IEEE Circuits Syst. Mag., vol.19, no.1, pp.33–54, 2019.
[9] G. Li and M. Gevers, "Roundoff noise minimization using delta-operator realizations," IEEE Trans. Signal Process., vol.41, no.2, pp.629–637, Feb. 1993.
[10] K. Premaratne, M.M. Ekanayake, J.I. Suarez, and P.H. Bauer, "Two-dimensional delta-operator formulated discrete-time systems: State-space realization and its coefficient sensitivity properties," IEEE Trans. Signal Process., vol.46, no.12, pp.3445–3449, Dec. 1998.
[11] J. Kauraniemi, T.I. Laakso, I. Hartimo, and S.J. Ovaska, "Delta operator realizations of direct-form IIR filters," IEEE Trans. Circuits Syst. II, Analog Digit. Signal Process., vol.45, no.1, pp.41–52, Jan. 1998.
[12] N. Wong and T.-S. Ng, "Roundoff noise minimization in a modified direct-form delta operator IIR structure," IEEE Trans. Circuits Syst. II, Analog Digit. Signal Process., vol.47, no.12, pp.1533–1536, Dec. 2000.
[13] N. Wong and T.-S. Ng, "A generalized direct-form delta operator-based IIR filter with minimum noise gain and sensitivity," IEEE Trans. Circuits Syst. II, Analog Digit. Signal Process., vol.48, no.4, pp.425–431, April 2001.
[14] G. Li and Z. Zhao, "On the generalized DFIIt structure and its state-space realization in digital filter implementation," IEEE Trans. Circuits Syst. I, Reg. Papers, vol.51, no.4, pp.769–778, April 2004.
[15] I.-H. Khoo, H.C. Reddy and P.K. Rajan, "Symmetry study for delta-operator-based 2-D digital filters," IEEE Trans. Circuits Syst. I, Reg. Papers, vol.53, no.9, pp.2036–2047, Sept. 2006.
[16] I.-H. Khoo, H.C. Reddy, and P.K. Rajan, "Efficient design of delta operator based 2-D IIR filters using symmetrical decomposition," Proc. 2008 IEEE Int. Symp. Circuits Syst. (ISCAS 2008), pp.700–703, Seattle, Washington, May 2008.
[17] I.-H. Khoo, H.C. Reddy, L.-D. Van, and C.T. Lin, "Delta operator based 2-D VLSI filter structures without global broadcast and incorporation of the quadrantal symmetry," Proc. 2012 IEEE Int. Symp. Circuits Syst. (ISCAS 2012), pp.3190–3193, Seoul, Korea, May 2012.
[18] C. Huang, H. Xu, Y. Chen, H. Song, and J. Zhang, "A new delta operator based IIR lattice filter structure," Proc. 2015 IEEE Int. Conf. Digital Signal Process. (DSP 2015), pp.44–47, Singapore, July 2015.
[19] M. Kawamata and T. Higuchi, "Synthesis of 2-D separable denominator digital filters with minimum roundoff noise and no overflow oscillations," IEEE Trans. Circuits Syst., vol.CAS-33, no.4, pp.365–372, April 1986.
[20] W.-S. Lu and A. Antoniou, "Synthesis of 2-D state-space fixed-point digital-filter structures with minimum roundoff noise," IEEE Trans. Circuits Syst., vol.CAS-33, no.10, pp.965–973, Oct. 1986.
[21] M.M. Ekanayake and K. Premaratne, "Two-dimensional delta-operator formulated discrete-time systems: Analysis and synthesis of minimum roundoff noise realizations," Proc. 1996 IEEE Int. Symp. Circuits Syst. (ISCAS 1996), vol.2, pp.213–216, Atlanta, GA, May 1996.
[22] T. Hinamoto, A. Doi, and W.-S. Lu, "Jointly optimal high-order error feedback and realization for roundoff noise minimization in 1-D and 2-D state-space digital filters," IEEE Trans. Signal Process., vol.61, no.23, pp.5893–5904, Dec. 2013.
[23] T. Hinamoto, A. Doi, and W.-S. Lu, "Roundoff noise minimization for 2-D separable-denominator digital filters using jointly optimal high-order error feedback and realization," Proc. 2017 IEEE Int. Symp. Circuits Syst. (ISCAS 2017), pp.2537–2540, Baltimore, MD, May 2017.
[24] T. Hinamoto, A. Doi, and W.-S. Lu, "Generalized direct-form II realization of 2-D separable-denominator digital filters," Proc. 2018 IEEE Int. Symp. Circuits Syst. (ISCAS 2018), Florence, Italy, May 2018.
[25] T. Hinamoto, A. Doi, and W.-S. Lu, "Roundoff noise analysis for generalized direct-form II structure of 2-D separable-denominator digital filters," Proc. 2018 26th European Signal Process. Conf. (EUSIPCO 2018), pp.455–459, Roma, Italy, Aug. 2018.
[26] R.P. Roesser, "A discrete state-space model for linear image processing," IEEE Trans. Autom. Control, vol.AC-20, no.1, pp.1–10, Feb. 1975.
[27] S.-Y. Kung, B.C. Levy, M. Morf, and T. Kailath, "New results in 2-D systems theory, Part II: 2-D state-space models — Realization and the notions of controllability, observability, and minimality," Proc. IEEE, vol.65, no.6, pp.945–961, June 1977.

Appendix: Roundoff Noise Measure for Filter Structure in (10)

We begin by examining the roundoff noise caused by the term $\alpha_k y(i,j)$ for $1 \le k \le m$ at the output. Due to the product quantization, for the actual filter implemented by a FWL system, (11) can be written as

$$
\begin{aligned}
\tilde{y}(i,j) &= \tilde{w}_1(i,j) + \sum_{l=1}^{n} r_{0l} x_l^v(i,j) \\
&\quad + r_{00}\Big[u(i,j) - \sum_{l=1}^{n} \beta_l x_l^v(i,j)\Big] \\
\tilde{w}_{k-1}(i,j) &= \rho_{k-1}^h(z_1)^{-1}\Big\{\tilde{w}_k(i,j) + \sum_{l=1}^{n} r_{k-1,l} x_l^v(i,j) \\
&\quad + r_{k-1,0}\Big[u(i,j) - \sum_{l=1}^{n} \beta_l x_l^v(i,j)\Big] - \alpha_{k-1}\tilde{y}(i,j)\Big\} \\
\tilde{w}_k(i,j) &= \rho_k^h(z_1)^{-1}\Big\{\tilde{w}_{k+1}(i,j) + \sum_{l=1}^{n} r_{kl} x_l^v(i,j) \\
&\quad + r_{k0}\Big[u(i,j) - \sum_{l=1}^{n} \beta_l x_l^v(i,j)\Big] - \big[\alpha_k \tilde{y}(i,j) + \overline{\varepsilon}_k(i,j)\big]\Big\} \\
\tilde{w}_{k+1}(i,j) &= \rho_{k+1}^h(z_1)^{-1}\Big\{\tilde{w}_{k+2}(i,j) + \sum_{l=1}^{n} r_{k+1,l} x_l^v(i,j) \\
&\quad + r_{k+1,0}\Big[u(i,j) - \sum_{l=1}^{n} \beta_l x_l^v(i,j)\Big] - \alpha_{k+1}\tilde{y}(i,j)\Big\}
\end{aligned}
\tag{A·1}
$$

where $\tilde{w}_0(i,j) = \tilde{w}_{m+1}(i,j) = 0$, $\tilde{y}(i,j)$ is the actual output of $y(i,j)$, $\tilde{w}_k(i,j)$ is the actual signal of $w_k(i,j)$, and

$$\overline{\varepsilon}_k(i,j) = Q[\alpha_k \tilde{y}(i,j)] - \alpha_k \tilde{y}(i,j)$$

is the roundoff noise due to quantizer $Q[\cdot]$. Subtracting (11) from (A·1) yields

$$\begin{aligned}
\delta y(i,j) &= \delta w_1(i,j)\\
\delta w_{k-1}(i,j) &= \rho_{k-1}^h(z_1)^{-1}\left[\delta w_k(i,j) - \alpha_{k-1}\delta y(i,j)\right]\\
\delta w_k(i,j) &= \rho_k^h(z_1)^{-1}[\delta w_{k+1}(i,j) - \alpha_k \delta y(i,j) - \overline{\varepsilon}_k(i,j)]\\
\delta w_{k+1}(i,j) &= \rho_{k+1}^h(z_1)^{-1}\left[\delta w_{k+2}(i,j) - \alpha_{k+1}\delta y(i,j)\right]
\end{aligned} \tag{A·2}$$

where

$$\begin{aligned}
\delta y(i,j) &= \tilde{y}(i,j) - y(i,j)\\
\delta w_k(i,j) &= \tilde{w}_k(i,j) - w_k(i,j)\\
&= \overline{\Delta}_k\left[\tilde{x}_k^h(i,j) - x_k^h(i,j)\right] = \overline{\Delta}_k\, \delta x_k^h(i,j)
\end{aligned}$$

By comparing (A·2) with (11), it is seen that the transfer function from $-\overline{\varepsilon}_k(i,j)$ to $\delta y(i,j)$ is given by

$$H_{1k}(z_1) = \boldsymbol{c}_1(z_1\boldsymbol{I}_m - \boldsymbol{A}_1)^{-1}\overline{\boldsymbol{e}}_k \quad \text{for} \quad k = 1,2,\cdots,m \tag{A·3}$$

where $\overline{\boldsymbol{e}}_k$ denotes the kth column of an identity matrix $\boldsymbol{I}_m$ of dimension $m \times m$. Based on above analysis, it appears to be rational to define the normalized noise gain in terms of $H_{1k}(z_1)$ as

$$J_1(\alpha_k) = \frac{E[\delta y(i,j)^2]}{E[\overline{\varepsilon}_k(i,j)^2]} = \frac{1}{2\pi j}\oint_{|z_1|=1} H_{1k}^H(z_1)\, H_{1k}(z_1)\frac{dz_1}{z_1} \tag{A·4}$$

where $H_{1k}^H(z_1)$ denotes the conjugate transpose of $H_{1k}(z_1)$. Substituting (A·3) into (A·4) yields

$$J_1(\alpha_k) = \overline{\boldsymbol{e}}_k^T \boldsymbol{W}^h \overline{\boldsymbol{e}}_k \quad \text{for} \quad k = 1,2,\cdots,m \tag{A·5}$$

where $\boldsymbol{W}^h$ is the horizontal observability Grammian in (24b). Similarly, the roundoff noise gain produced by the coefficient r_{kl} for $l = 0,1,\cdots,n$ in the second equation of (11) can be expressed as

$$J_2(r_{kl}) = \overline{\boldsymbol{e}}_k^T \boldsymbol{W}^h \overline{\boldsymbol{e}}_k \quad \text{for} \quad k = 1,2,\cdots,m \tag{A·6}$$

With $w_{k+1}(i,j)$ replaced by $\overline{\Delta}_{k+1}x_{k+1}^h(i,j)$ in the second equation of (11), the roundoff noise gain due to $\overline{\Delta}_{k+1}$ can be viewed as a function of r_{kl}, i.e.,

$$J_2(\overline{\Delta}_{k+1}) = J_2(r_{kl}) = \overline{\boldsymbol{e}}_k^T \boldsymbol{W}^h \overline{\boldsymbol{e}}_k \quad \text{for} \quad k = 1,2,\cdots,m-1 \tag{A·7}$$

As shown in Fig. 1(a), parameter $\overline{\gamma}_k$ induces a multiplication $\overline{\gamma}_k x_k^h(i,j)$ which produces no roundoff noise if $\overline{\gamma}_k = 0$, ± 1. Let $\psi(\overline{\gamma}_k)\epsilon_k^h(i,j)$ denote the roundoff noise due to $\overline{\gamma}_k$ where $\psi(\overline{\gamma}_k) = 1$ for all $\overline{\gamma}_k$ except $\overline{\gamma}_k = 0, \pm 1$ for which $\psi(\overline{\gamma}_k) = 0$, and $\delta y(i,j)$ be the corresponding output deviation. Then the transfer function from $\psi(\overline{\gamma}_k)\epsilon_k^h(i,j)$ to $\delta y(i,j)$ becomes $H_{1k}(z_1)$ in (A·3). Actually, this roundoff noise can be viewed as that generated by the term $r_{kl}x_l^v(i,j)$. Hence the roundoff noise gain in question is given by

$$J_3(\overline{\gamma}_k) = \psi(\overline{\gamma}_k)J_2(r_{kl}) = \psi(\overline{\gamma}_k)\overline{\boldsymbol{e}}_k^T \boldsymbol{W}^h \overline{\boldsymbol{e}}_k \tag{A·8}$$

for $k = 1,2,\cdots,m$ where $\psi(\gamma)$ is defined as in (25).

Concerning the roundoff noise due to coefficient r_{0l} for $l = 0,1,\cdots,n$ in the first equation of (11), the first equation in (A·2) needs to be changed to

$$\delta y(i,j) = \delta w_1(i,j) + \varepsilon_{0l}(i,j) \tag{A·9}$$

where $\varepsilon_{0l}(i,j)$ is the roundoff noise caused by r_{0l}. Suppose a state-space model is realized from (A·9) and the remaining part of (A·2) with $\overline{\varepsilon}_k(i,j) = 0$ by referring to (13c) and (14), the transfer function from $\varepsilon_{0l}(i,j)$ to $\delta y(i,j)$ is given by

$$H_{10}(z_1) = -\boldsymbol{c}_1(z_1\boldsymbol{I}_m - \boldsymbol{A}_1)^{-1}\boldsymbol{\alpha} + 1 \tag{A·10}$$

where $\boldsymbol{\alpha} = [\alpha_1, \alpha_2, \cdots, \alpha_m]^T$. Hence the roundoff noise gain caused by coefficient r_{0l} is found to be

$$J_4(r_{0l}) = \boldsymbol{\alpha}^T \boldsymbol{W}^h \boldsymbol{\alpha} + 1 \quad \text{for} \quad l = 0,1,\cdots,n \tag{A·11}$$

Supposing that $w_1(i,j)$ in the first equation of (11) is replaced by $\overline{\Delta}_1 x_1^h(i,j)$, it is seen that the roundoff noise gain produced by $\overline{\Delta}_1$ is identical to that by r_{0l}, which leads to

$$J_4(\overline{\Delta}_1) = J_4(r_{0l}) = \boldsymbol{\alpha}^T \boldsymbol{W}^h \boldsymbol{\alpha} + 1 \tag{A·12}$$

We now examine the roundoff noise caused by the term $\beta_p x_p^v(i,j)$ for $1 \le p \le n$ at the output. Due to the product quantization, for the actual filter implemented by a FWL system, (11) and (12) can be written as

$$\begin{aligned}
\tilde{y}(i,j) &= \tilde{w}_1(i,j) + \sum_{l=1}^{n} r_{0l}\tilde{x}_l^v(i,j)\\
&\quad + r_{00}\Big[u(i,j) - \sum_{l=1}^{n}\beta_l\tilde{x}_l^v(i,j) - \hat{\varepsilon}_p(i,j)\Big]\\
\tilde{w}_k(i,j) &= \rho_k^h(z_1)^{-1}\Big\{\tilde{w}_{k+1}(i,j) + \sum_{l=1}^{n} r_{kl}\tilde{x}_l^v(i,j)\\
&\quad + r_{k0}\Big[u(i,j) - \sum_{l=1}^{n}\beta_l\tilde{x}_l^v(i,j) - \hat{\varepsilon}_p(i,j)\Big] - \alpha_k\tilde{y}(i,j)\Big\}
\end{aligned} \tag{A·13}$$

for $k = 1,2,\cdots,m$ where $\tilde{w}_{m+1}(i,j) = 0$, and

$$\begin{aligned}
\tilde{x}_1^v(i,j+1) &= \hat{\gamma}_1\tilde{x}_1^v(i,j)\\
&\quad + \hat{\Delta}_1\Big[u(i,j) - \sum_{l=1}^{n}\beta_l\tilde{x}_l^v(i,j) - \hat{\varepsilon}_p(i,j)\Big]\\
\tilde{x}_l^v(i,j+1) &= \hat{\Delta}_l\tilde{x}_{l-1}^v(i,j) + \hat{\gamma}_l\tilde{x}_l^v(i,j)
\end{aligned} \tag{A·14}$$

for $l = 2, 3, \cdots, n$, respectively, where $\tilde{x}_l^v(i,j)$ denotes the actual signal of $x_l^v(i,j)$ and

$$\hat{\varepsilon}_p(i,j) = Q[\beta_p \tilde{x}_p^v(i,j)] - \beta_p \tilde{x}_p^v(i,j)$$

is the roundoff noise due to quantizer $Q[\,\cdot\,]$. Subtracting (11) from (A· 13) yields

$$\begin{aligned}\delta y(i,j) &= \delta w_1(i,j) + \sum_{l=1}^{n} r_{0l}\delta x_l^v(i,j) \\ &\quad + r_{00}\Big[-\hat{\varepsilon}_p(i,j) - \sum_{l=1}^{n}\beta_l \delta x_l^v(i,j)\Big] \\ \delta w_k(i,j) &= \rho_k^h(z_1)^{-1}\Big\{\delta w_{k+1}(i,j) + \sum_{l=1}^{n} r_{kl}\delta x_l^v(i,j) \\ &\quad + r_{k0}\Big[-\hat{\varepsilon}_p(i,j) - \sum_{l=1}^{n}\beta_l\delta x_l^v(i,j)\Big] - \alpha_k \delta y(i,j)\Big\}\end{aligned} \tag{A· 15}$$

for $k = 1, 2, \cdots, m$ where $\delta w_{m+1}(i,j) = 0$ and

$$\delta x_l^v(i,j) = \tilde{x}_l^v(i,j) - x_l^v(i,j) \quad \text{for } l = 1, 2, \cdots, n$$

By subtracting (12) from (A· 14), we obtain

$$\begin{aligned}\delta x_1^v(i,j+1) &= \hat{\gamma}_1 \delta x_1^v(i,j) + \hat{\Delta}_1\Big[-\hat{\varepsilon}_p(i,j) - \sum_{l=1}^{n}\beta_l \delta x_l^v(i,j)\Big] \\ \delta x_l^v(i,j+1) &= \hat{\Delta}_l \delta x_{l-1}^v(i,j) + \hat{\gamma}_l \delta x_l^v(i,j)\end{aligned} \tag{A· 16}$$

At this point, we consider the local state-space realization of (A· 15) and (A· 16). By comparing (A· 15) with (11) and (A· 16) with (12), respectively, it follows that the transfer function from $-\hat{\varepsilon}_p(i,j)$ to $\delta y(i,j)$ is given by (15).

Based on this, the roundoff noise gain is expressed in terms of $H(z_1, z_2)$ as

$$\begin{aligned}J_5(\beta_p) &= \frac{E[\delta y(i,j)^2]}{E[\hat{\varepsilon}_p(i,j)^2]} \\ &= \frac{1}{(2\pi j)^2}\oint_{|z_1|=1}\oint_{|z_2|=1} H^H(z_1,z_2)\, H(z_1,z_2)\frac{dz_1 dz_2}{z_1 z_2}\end{aligned} \tag{A· 17}$$

Substituting (15) into (A· 17) yields

$$J_5(\beta_p) = \boldsymbol{b}_1^T \boldsymbol{W}^h \boldsymbol{b}_1 + \boldsymbol{b}_2^T \boldsymbol{W}^v \boldsymbol{b}_2 + d^2 \tag{A· 18}$$

where $\boldsymbol{W}^v$ is the vertical observability Grammian in (24b).

Due to the product quantization caused by $\hat{\Delta}_1$ in the first equation of (12), the actual filter implemented by a FWL system can be written from (11) and (12) as

$$\begin{aligned}\tilde{y}(i,j) &= \tilde{w}_1(i,j) + \sum_{l=1}^{n} r_{0l}\tilde{x}_l^v(i,j) \\ &\quad + r_{00}\Big[u(i,j) - \sum_{l=1}^{n}\beta_l \tilde{x}_l^v(i,j)\Big] \\ \tilde{w}_k(i,j) &= \rho_k^h(z_1)^{-1}\Big\{\tilde{w}_{k+1}(i,j) + \sum_{l=1}^{n} r_{kl}\tilde{x}_l^v(i,j) \\ &\quad + r_{k0}\Big[u(i,j) - \sum_{l=1}^{n}\beta_l \tilde{x}_l^v(i,j)\Big] - \alpha_k \tilde{y}(i,j)\Big\}\end{aligned} \tag{A· 19}$$

for $k = 1, 2, \cdots, m$ where $\tilde{w}_{m+1}(i,j) = 0$, and

$$\begin{aligned}\tilde{x}_1^v(i,j+1) &= \hat{\gamma}_1 \tilde{x}_1^v(i,j) + \hat{\Delta}_1\Big[u(i,j) - \sum_{l=1}^{n}\beta_l \tilde{x}_l^v(i,j)\Big] \\ &\quad + \varepsilon_1^v(i,j) \\ \tilde{x}_l^v(i,j+1) &= \hat{\Delta}_l \tilde{x}_{l-1}^v(i,j) + \hat{\gamma}_l \tilde{x}_l^v(i,j)\end{aligned} \tag{A· 20}$$

for $l = 2, 3, \cdots, n$, respectively, where $\varepsilon_1^v(i,j)$ is the roundoff noise caused by $\hat{\Delta}_1$. Subtracting (11) from (A· 19) yields

$$\begin{aligned}\delta y(i,j) &= \delta w_1(i,j) + \sum_{l=1}^{n} r_{0l}\delta x_l^v(i,j) - r_{00}\sum_{l=1}^{n}\beta_l \delta x_l^v(i,j) \\ \delta w_k(i,j) &= \rho_k^h(z_1)^{-1}\Big\{\delta w_{k+1}(i,j) + \sum_{l=1}^{n} r_{kl}\delta x_l^v(i,j) \\ &\quad - r_{k0}\sum_{l=1}^{n}\beta_l \delta x_l^v(i,j) - \alpha_k \delta y(i,j)\Big\}\end{aligned} \tag{A· 21}$$

for $k = 1, 2, \cdots, m$ where $\delta w_{m+1}(i,j) = 0$. Subtracting (12) from (A· 20), we obtain

$$\begin{aligned}\delta x_1^v(i,j+1) &= \hat{\gamma}_1 \delta x_1^v(i,j) - \hat{\Delta}_1 \sum_{l=1}^{n}\beta_l \delta x_l^v(i,j) + \varepsilon_1^v(i,j) \\ \delta x_l^v(i,j+1) &= \hat{\Delta}_l \delta x_{l-1}^v(i,j) + \hat{\gamma}_l \delta x_l^v(i,j)\end{aligned} \tag{A· 22}$$

for $l = 2, 3, \cdots, n$, respectively. Since (14) is derived from (11) and (12) by using (13c), it follows from (A· 21) and (A· 22) that the transfer function from $\varepsilon_1^v(i,j)$ to $\delta y(i,j)$ is given by (15) with $\boldsymbol{b}_1 = \boldsymbol{0}$, $\boldsymbol{b}_2 = \hat{\boldsymbol{e}}_1$ and $d = 0$ as

$$H_{21}(z_1, z_2) = [\boldsymbol{c}_1(z_1\boldsymbol{I}_m - \boldsymbol{A}_1)^{-1}\boldsymbol{A}_2 + \boldsymbol{c}_2](z_2\boldsymbol{I}_n - \boldsymbol{A}_4)^{-1}\hat{\boldsymbol{e}}_1 \tag{A· 23}$$

where $\hat{\boldsymbol{e}}_l$ denotes the lth column of an identity matrix $\boldsymbol{I}_n$. Hence the roundoff noise gain due to $\hat{\Delta}_1$ becomes

$$J_6(\hat{\Delta}_1) = \hat{\boldsymbol{e}}_1^T \boldsymbol{W}^v \hat{\boldsymbol{e}}_1 \tag{A· 24}$$

Similarly, the roundoff noise gain due to $\hat{\Delta}_l$ for $l = 2, 3, \cdots, n$ is given by

$$J_6(\hat{\Delta}_l) = \hat{\boldsymbol{e}}_l^T \boldsymbol{W}^v \hat{\boldsymbol{e}}_l \quad \text{for } l = 2, 3, \cdots, n \tag{A· 25}$$

and the roundoff noise gain due to $\hat{\gamma}_l$ for $l = 1, 2, \cdots, n$ can be written as

$$J_6(\hat{\gamma}_l) = \psi(\hat{\gamma}_l)\hat{\boldsymbol{e}}_l^T \boldsymbol{W}^v \hat{\boldsymbol{e}}_l \quad \text{for } l = 1, 2, \cdots, n \tag{A· 26}$$

Based on the above analysis, the roundoff noise measure for the filter structure in (10) can be defined as

$$\begin{aligned}J_\rho &= \sum_{k=1}^{m}\Big[J_1(\alpha_k) + \sum_{l=0}^{n} J_2(r_{kl}) + J_3(\overline{\gamma}_k)\Big] \\ &\quad + \sum_{k=1}^{m-1} J_2(\overline{\Delta}_{k+1}) + J_4(\overline{\Delta}_1) + J_4(r_{00}) \\ &\quad + \sum_{l=1}^{n}\Big[J_4(r_{0l}) + J_5(\beta_l) + J_6(\hat{\Delta}_l) + J_6(\hat{\gamma}_l)\Big]\end{aligned} \tag{A· 27}$$

which can be written as in (27).

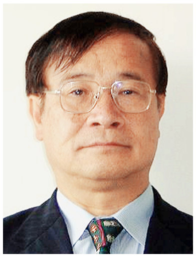

Takao Hinamoto received the B.E. degree from Okayama University, Okayama, Japan, in 1969, the M.E. degree from Kobe University, Kobe, Japan, in 1971, and the Dr. Eng. degree from Osaka University, Osaka, Japan, in 1977, all in electrical engineering. From 1972 to 1988, he was with the Faculty of Engineering, Kobe University, Kobe, Japan. From 1979 to 1981, he was a Visiting Member of Staff in the Department of Electrical Engineering, Queen's University, Kingston, ON, Canada, on leave from Kobe University. During 1988–1991, he was Professor of Electronic Circuits in the Faculty of Engineering, Tottori University, Tottori, Japan. During 1992–2009, he was Professor of Electronic Control in the Department of Electrical Engineering, Hiroshima University, Hiroshima, Japan. Since 2009, he has been a Professor Emeritus of Hiroshima University. His research interests include digital signal processing, system theory, and control engineering. He has published over 400 papers in these areas. He is the co-editor and co-author of *Two-Dimensional Signal and Image Processing* (SICE, 1996) and the co-author with W.-S. Lu of *Digital Filter Design and Realization* (River Publishers, 2017). Dr. Hinamoto is a Life Fellow of the IEEE and a Fellow of the Society of Instrument and Control Engineers (SICE).

Akimitsu Doi received the B.E. degree in Electronic Engineering from Tottori University in 1992, and M.E. and Ph.D. degrees in System Engineering from Hiroshima University in 1994 and 1997, respectively. From 1997 to 2002, he was a Research Associate with the Faculty of Engineering, Hiroshima University, Hiroshima, Japan. From 2002 to 2005, he was a Lecturer in the Faculty of Engineering, Hiroshima Institute of Technology, Hiroshima, Japan. From 2005 to 2015, he was an Associate Professor and since October 2015, he has been a Professor at the same Institute. His research interests are in the area of digital signal and image processing.

Wu-Sheng Lu received his undergraduate degree in mathematics from Fudan University, Shanghai, China, in 1964, the M.S. degree in electrical engineering, and the Ph.D. degree in control science from University of Minnesota, Minneapolis, USA, in 1983 and 1984, respectively. He was a post-doctoral fellow at University of Victoria, Victoria, B.C., Canada, in 1985, and a visiting assistant professor at University of Minnesota from January 1986 to April 1987. Since May 1987, he has been with the Electrical and Computer Engineering Department, University of Victoria where he is a professor. His current research interests include analysis and design of digital filters, signal and image processing, and methods of convex optimization. He is the co-author with A. Antoniou of Two-Dimensional Digital Filters (Marcel Dekker, 1992) and Practical Optimization: Algorithms and Engineering Applications (Springer, 2007). Dr. Lu served as editor for the Canadian Journal of Electrical and Computer Engineering and associate editor for several journals including IEEE Transactions on Circuits and Systems I and II, International Journal of Multidimensional Systems and Signal Processing, and Journal of Circuits, Systems, and Signal Processing. Dr. Lu is a Life Fellow of the IEEE, a Fellow of the Engineering Institute of Canada, and a registered professional engineer in British Columbia, Canada.